AD

TECHNICAL REPORT ECOM-00032-F

INVESTIGATION OF THE QUANTITATIVE DETERMINATION OF POINT AND AREAL PRECIPITATION BY RADAR ECHO MEASUREMENTS

FINAL REPORT

by

E. A. Mueller - A. L. Sims

December 1966

ECOM

UNITED STATES ARMY ELECTRONICS COMMAND · FORT MONMOUTH, N J.

ATMOSPHERIC SCIENCES LABORATORY

Contract DA-28-043 AMC-00032(E)
ILLINOIS STATE WATER SURVEY
at the
University of Illinois
Urbana, Illinois

NOTICES

Disclaimers

The findings in this report are not to be construed as an official Department of the Army position, unless so designated by other authorized documents.

The citation of trade names and names of manufacturers in this report is not to be construed as official Government indorsement or approval of commercial products or services referenced herein.

Disposition

Destroy this report when it is no longer needed. Do not return it to the originator.

RCS OSD-1366

TECHNICAL REPORT ECOM-00032-P December 1966

INVESTIGATION OP THE QUANTITATIVE DETERMINATION OP POINT AND AREAL PRECIPITATION BY RADAR ECHO MEASUREMENTS

PINAL REPORT

1 October 1964 to 30 September 1966

Contract No. DA-28-043 AMC-00032 (E)
DA Pro ject No. lVO-14501-B-53A-07

Prepared by

E. A. Mueller and A. L. Sims

ILLINOIS STATE WATER SURVEY
at the
University of Illinois
Urbana, Illinois

for

U. S. ARMY ELECTRONICS COMMAND, PORT MONMOUTH, N.J.

ABSTRACT

A review of work accomplished on this contract is presented including references to the appropriate interim reports for details. The limiting accuracy for radar estimation of rainfall rate is determined to be about ± 40 percent.

The location of the medium range raingage network is shown along with the amount of data collected thus far. No results from this network are available at present.

A Doctoral thesis entitled, "Radar Cross Sections from Drop Size Spectra," is included as an Appendix.

CONTENTS

THE ACCURACY OF RAINFALL MEASUREMENT BY RADAR

Drop Size Spectra Accuracy Limitations

A large portion of the effort on this contract was directed toward assessing the accuracy with which radar can determine rainfall amounts. A number of separate efforts to this end have been pursued. Fundamental to the ability to measure precipitation amounts is the relationship between the radar cross section and the rainfall rate. This relationship is dependent on the raindrop size distribution. Measurements of many spectra have been made under prior Army sponsorship in various climatic areas. Relationships have been developed from these spectra. The uncertainty in these relationships when corrected for errors of sample size, produce bounds on the accuracy of rainfall rates. It is true, however, that if amounts are desired rather than rates an additional improvement will be possible through reduction of the scatter with time integration. A presentation of the drop-size limited accuracy in estimation of rainfall rates is presented in Interim Report No. 3, Page 13.

The appendix to this report is a doctoral thesis which presents in one place a summary of radar-rainfall relationships. Briefly, the drop size data suggest that the 90% confidence level is some 43% from the mean. This can be improved in some cases and in some areas by using additional information such as rain type, synoptic type, or thermodynamic instability. In some cases the rate may be estimated to within 35% by these stratifications. With Oregon thunderstorms, this measurement accuracy improves to 25%, but

this is believed to be primarily due to limited sample size and is not considered a representative estimate.

When values of rainfall rate are transformed to radar parameters, they suggest that the overall calibration and measurement accuracy of the radar must be known to within 2 decibels in order to have the radar measurement error of the same size as the uncertainty in drop size. Unless the radar power return is averaged over more than 10 independent samples, this accuracy is unachievable.[1] According to Smith, 10 samples will produce a distribution which is 2 db wide at 90% confidence points.

Radar parameters, particularly the antenna gain, are seldom known or measureable to within this accuracy. Thus, it would appear that with present technology that radar rainfall rate estimates will, in general, be much less than predicted from drop size distributions.

Radar-Rainfall Accuracy as a Function of Range

No additional inaccuracy of rainfall rate estimates due to drop size variability is expected in range. However, the height at which the radar views the storm does vary greatly with range. It is obvious that if the sampling height is sufficiently high the estimate of rain is meaningless. To evaluate the loss in accuracy as the range from the radar increases, a raingage network was installed in the northern part of the state of Illinois during May of 1966. Results of this study are not yet available (see section on Kankakee Network)

FREQUENCY OP OCCURRENCES OP RAINFALL RATES

As a part of this contract, statistics of rainfall rates were obtained. The primary intent of this work is to provide design information for communication equipment at attenuating wavelengths. Two methods were chosen for this study. In the first method, merely the frequency distributions of point rates were obtained. In the second, network data were used to permit evaluation of a combination of the path length and severity of the rainfall on attenuation. Results have been presented in the three Interim reports on this contract. In the second interim report the network data are presented. These data are not as complete as desired as the analysis time to obtain the raingage rates were greater than anticipated. During the coming months this analysis will be extended by including more data.

Attempts to locate suitable network raingage data from other areas have been unsuccessful. In order to be reasonably useful the network data has to be such that 5-minute amounts can be determined reliably.

Individual raingage statistics from Bogor, Indonesia; Miami, Florida; and Illinois have been presented in the interim reports. Considerable differences in these statistics are indicated. At the 0.1% of time level, Indonesia exhibits the highest rainfall rate. However, at the 1% time level, Florida has the highest rate. In all cases Illinois has the lowest rainfall rate. Table 1 illustrates the frequencies of rainfall rates at these locations and indicates the approximate 3-cm wavelength attenuation that would be experienced at each interval.

TABLE 1

FREQUENCY OP RAINFALL RATE OCCURRENCES
IN DIFFERENT CLIMATIC REGIMES

Location	Rainfall Rate (in/hr)	% of rain time the rate is exceeded	Attenuation (db/mile)
Bogor Indonesia	6.5	.1	8.7
	3.2	1.0	3.7
	1.0	10.0	.9
Miami, Florida	5.9	.1	7.7
	3.8	1.0	4.5
	1.2	10.0	1.1
Champaign, Ill.	3.3	.1	3.8
	1.8	1.0	1.8
	0.6	10.0	.48

DROP SIZE SPECTRA

Log Normal Distributions

An important scientific result of the work with drop size spectra is the finding that the best fitting equation for drop size spectra is the log normal equation. This is reported in Interim Report No. 1. This result should be very useful for studies involving the processes by which cloud droplets grow to, rain drops.

Sample Size Studies

A large part of the effort in recent months has been to evaluate the representativeness of the drop size spectra. Results have been reported in the Interim reports and also in the paper

delivered at the 1966 Radar Meteorology Conference in Norman, Oklahoma. The results of this study indicate that for the usual radars, no errors due to the sampling volume being too small will occur. The variance in estimated rainfall rate due to a one-cubic-meter sample represents only about 10% of the total sample variance around the regression.

Flagstaff, Arizona Drop-size Data

The measurement and analysis of drop-size data obtained this summer in Flagstaff, Arizona under Contract No. DA-28-043 AMC-02376(E) is continuing. Although only very preliminary results are available at this time, it appears that the Flagstaff rains contain more large drops than has generally been found at other locations.

THE KANKAKEE RAINGAGE NETWORK

The Kankakee Raingage Network was established in an area in and to the southeast of Kankakee, Illinois, in early April 1966. Fifteen recording raingages were received as government-furnished equipment. These are gages 2 through 16 on the map of figure 1. Gage 1 is the Weather Bureau gage at Kankakee. The gages are spaced at a distance of about 5 miles in a 4 x 4. grid.

Data were collected on this network from April 15 through September 30. The gages have now been removed for the winter and will be reinstalled in the spring. The data from this network is being used in connection with radar data to determine the accuracies of radar-rainfall measurements at a range of 65 nautical miles from the radar.

Table 2 shows some of the information concerning the storms which have been selected for detailed analysis. These storms all have at least 1/2-hour of concurrent radar-raingage data and have maximum single gage amounts of at least .05 inch. Tracings of the radar step-gain pictures have been completed for all but two of these storms. The areas of each step have been measured for about one-half of the data. Considerable work remains before definite conclusions can be made from these data.

TABLE 2

1966 STORMS AT THE KANKAKEE NETWORK BEING USED IN RADAR-RAINGAGE COMPARISONS

Date	Rain Period (gage)	Radar Data Period	Single Gage Maximum Amount (inches)	Mean Network Amount (inches)
4/20	1550-0132	11+35-1708	1.45	1.13
5/11-12	0100-0340	0705-2015	2.51	1.73
5/17	081+0-151+0	0715-1523	0.1+9	0.15
5/23-24	1900-0130	1341-2234	1.81;	1.37
6/8	1320-1620	0656- to	0.06	0.02
6/8-9	2150-0313	-0814	0.80	0.55
6/26	1415-1730	151+5- to	0.50	0.05
6/26	1910-2128	-2057	0.50	0.15
8/8	131+3-1532	11+30-191+1	0.31	0.05
8/10	001+8-2130	0700-1607	1.1+9	1.19
8/14	1425-1735	1251+-1945	0.58	0.02
8/21-22	1645-0100	1929-2139	0.93	0.51+
9/3	031+1+-1505	1221-121+0 & 1325-1536	0.18	0.03
9/11+	1200-21+00	0700-2221+	1.01	0.1+6
9/19	1500-2130	0824-1650	0.25	0.02

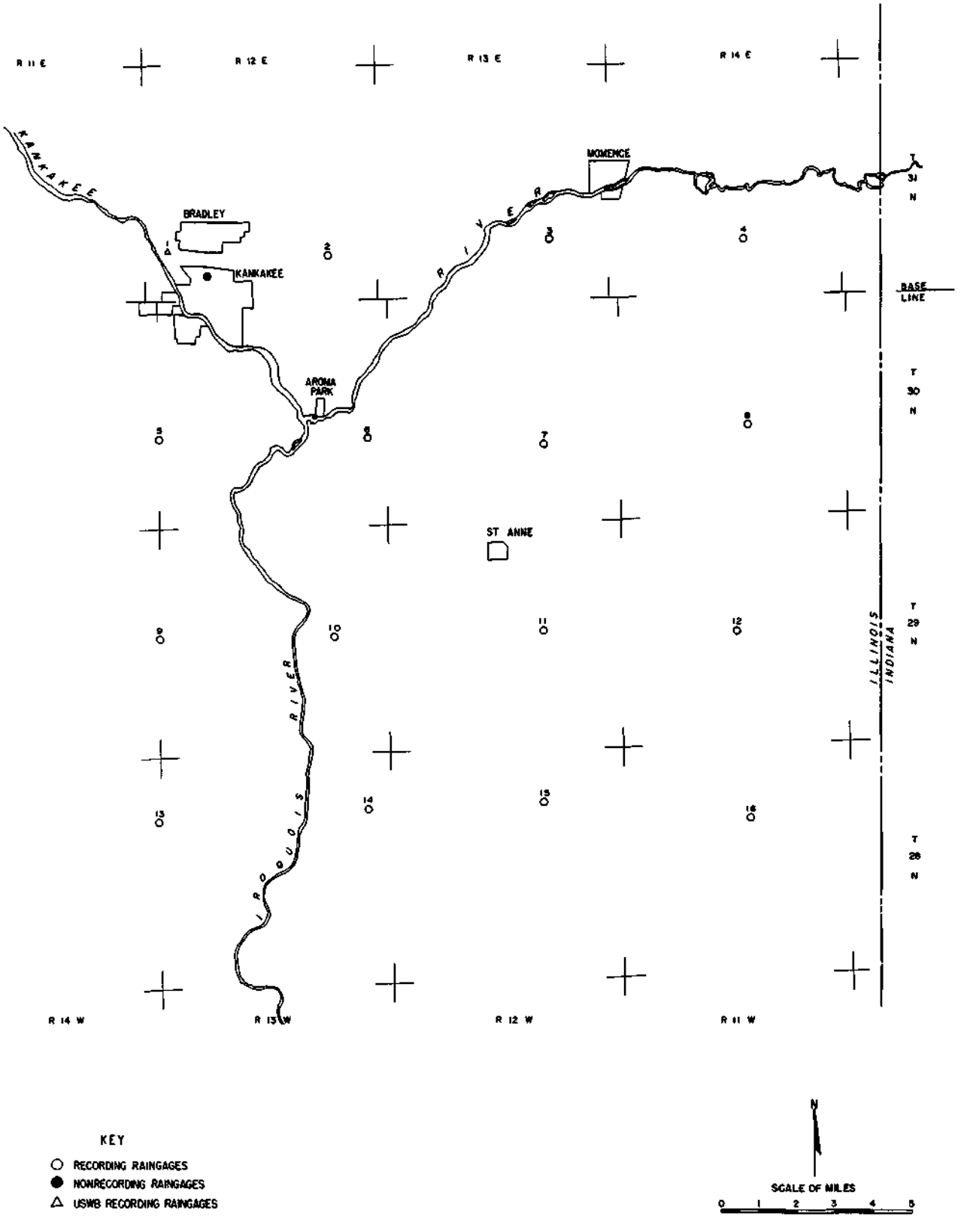

Figure 1. The Kankakee Raingage Network

RADAR OPERATIONS

The CPS-9 radar was operated a total of 490 hours during the period April 1, 1966, to September 30, 1966. Approximately 290 hours of this time were used in collecting data over the raingage networks. These data are in the form of stepped gain photographs. The data were collected for the purpose of rainfall-radar correlation with the raingage measurements from the raingage networks.

The M-33 acquisition system has also been used during most of the season. The maximum range of this radar has been increased to 80 nautical miles in order to observe rainfall over the Kankakee Network.

DROP-SIZE DATA REPORTS

Reports of drop-size data are being prepared for Ma juro, Marshall Islands; Franklin, North Carolina; Island Beach, New Jersey; Bogor, Indonesia; Corvallis, Oregon; and Woody Island, Alaska. The format for these reports was described in Interim Report No. 3. The draft report for Majuro, known as Research Report no. 10 has been submitted for Army approval. The tabulations of data have been completed for North Carolina and New Jersey. Much of the preliminary data checking has been done for the other locations.

CONCLUSIONS & RECOMMENDATIONS

The ability of a radar to measure rainfall rate is limited ultimately by the variability of the drop size distributions. The present state of the art in meteorological radar techniques

does not permit measurements of rainfall rate to the limits imposed by drop size distributions. Measurement of rainfall amounts can be made with sufficient accuracy that it would appear to be useful to the tactical operations of the Army.

Rainfall rate statistics have been processed to indicate the severity and frequency of occurrences of the attenuating rainfall rates for communications and radar operations at attenuating wavelengths. The interpretation of these statistics is highly dependent upon the character of the operation envisioned and thus have not been examined extensively. All other engineering and equipment portability considerations aside, the attenuation data do indicate the need for longer wavelength radars for measurement of rainfall rates and amounts by radar. An uncorrected error of size equivalent to the drop size uncertainty will occur about 20% of the rain time in central Illinois with 3-cm wavelength radar. As has been pointed out in previous reports, if a 3-cm radar is to be used for measuring rainfall rates or amounts, some correction for this attenuation is adviseable.

Future work should be directed toward the improvement of the radar instrumentation. In particular the integration of the radar data by automatic means is considered essential to measure meaningful radar rates. The evaluation of accuracy of rainfall rates as determined by radar using raingage networks must be continued. The Kankakee network should be reinstalled for the spring and summer season of 1967 and more data over this network obtained. At present it is felt that the accuracy at 75 miles using the CPS-9 will be reduced by about one-half order of magnitude. This would tend to dictate that the number of radar sets in an Army

tactical area should be about one set every 4000 square miles, if quantitative accuracy is to remain reasonable.

Drop size data reports should be issued for the remaining locations in the near future.

Additional analysis of drop size data with respect to other variables is desireable. For example, analysis of the radar-rainfall relationship using the rainfall rate as the independent variable may be of interest to the Army as an aid in designing non-meteorological radar. Other relationships such as rainfall limited visibility versus radar reflectivity, rainfall limited visibility versus rainfall rate, and liquid water content versus reflectivity might also be of importance.

REFERENCES

1. Smith, Paul L., Jr., 1964. Interpretation of the fluctuating distributed scatterers: Part 3. Report MW-39, Scientific report No. 1, APCRL Contract No. AP 19 (628)-2489, Stormy Weather Group, McGill University, Montreal, Canada.

APPENDIX

RADAR CROSS SECTIONS PROM DROP SIZE SPECTRA

BY

EUGENE ALBERT MUELLER

B.S., University of Illinois, 1951

M.S., University of Illinois, 1952

THESIS

Submitted in partial fulfillment of the requirements for the degree of Doctor of Philosophy in Electrical Engineering in the Graduate College of the University of Illinois, 1966

Urbana, Illinois

TABLE OP CONTENTS

LIST OF TABLES

LIST OF ILLUSTRATIONS

LIST OF SYMBOLS

σ	radar back scattering cross section
Q_t	radar attenuation cross section
λ	wavelength of the radiation
α	ratio of circumference of the sphere to wavelength
D	equivalent spherical diameter of raindrop
m	complex index of refraction
Z	radar reflectivity defined as the sum of sixth power of drop diameters in one cubic meter
L	liquid water content
N_D	number of drops of diameter D per cubic meter
N_T	total number of drops per cubic meter
R	rainfall rate
a	coefficient of the R-Z relationships
b	exponent of the R-Z relationships

ABSTRACT

The design of a raindrop camera to obtain the raindrop size spectrum is discussed. The camera is capable of sampling 1 m^3 of air space in 10.5 seconds. Within this volume the size of the raindrops are measured to an accuracy of ±0.2 mm.

The cameras were installed at Corvallis, Oregon; Miami, Florida; Woody Island, Alaska; Ma juro, Marshall Islands; Bogor, Indonesia; Franklin, North Carolina; and Island Beach, New Jersey. A sample of one year's duration was obtained at each location.

The drop size spectra for various rainfall rates have been determined, and it is shown that the logarithmic normal distribution Is the best descriptive equation for these spectra. The radar back scattering cross section was calculated and its relationship to the rainfall rate determined. The relationship varies from location to location. Alaska rains exhibit the largest back scattering cross section for a given rate. For some rates nearly 10 times more radar return can be anticipated from Alaska rain than from the tropical rains of the Marshall Islands.

The data has been stratified according to rain type, synoptic type, and thermodynamic instability. These stratifications improve the reliability with which the rainfall rate can be determined by radar measurements. The synoptic stratification reduces the uncertainty more than the other methods.

Liquid water content of rain was calculated and related to the rainfall rate. At Miami concentrations of 10 g/m^3 occur more than 1 percent of the rain time. Liquid water contents were higher in Miami than at any other location.

The radar attenuation cross section was calculated for some of the data and compared favorably with earlier estimates of attenuation by others.

INTRODUCTION

During World War II, many observations of rainstorms by radar were made. These were detrimental to the desired use of the radar and investigations into the nature of the scattering were conducted by Ryde[1] of General Electric and Bent[2] of the Radiation Laboratory of Massachusetts Institute of Technology along with others. This work indicated the need for knowledge of the drop size distributions which occur in rain. After the war, a number of groups interested primarily in meteorology began using radar as a tool in weather research. Until about 1947, most of the work with weather radar was directed towards locating the storms,, The first work in determining the rainfall rate from the radar return was performed by numerous groups in l947.[3,4,5,6,7] This work emphasized the need for better information on the drop size spectra.

Most of this early work consisted of measuring the radar parameters and comparing these measurements with rainfall rates as determined by raingages. By 1956, it was apparent that there was considerably greater error in the measured rainfall rates than could be tolerated for most uses. A number of possibilities exist that may contribute to this error. A raingage samples rainfall at a point and at best the radar samples a volume surrounding the raingage. Rain measured aloft with the radar may well drift a mile before it reaches the ground and thus fail to be caught in the raingage. Rain aloft may not be falling at all due to updrafts

supporting the raindrops. In addition to these problems which are related to catching the rainfall in a raingage, it was anticipated that different types of rains produce different amounts of radar return signals.

This latter problem is investigated theoretically by measuring the raindrop size spectra and calculating the radar return and the rainfall rate. Drop size spectra were obtained at seven locations outside of Illinois. These locations represent a sampling of all the rainy climatic types.

History of Drop Size Measurement

Raindrop sizes were measured in the latter part of the nineteenth century. Apparently, some interest had been generated by sailors returning from the tropics and reporting "raindrops as large as teacups." Lowe[9] was one of the earliest researchers in drop size measurement. His measurement was performed by allowing the drops to fall on ruled slate and measuring the size of the splash. This basic method can be categorized by the measurement of an image of a drop after impingement on a flat surface. The surfaces which have been used include dyed filter paper, blue print paper, treated photographic film and coated nylon screen. These methods are simple and use a minimum of equipment. Calibration of the devices is accomplished by dropping drops of known size on the surface and measuring the resultant traces. Large drops are difficult to measure since they splash on impact leaving irregular traces. As a result of the splashes, the possibility exists of over-estimating the

number of small drops due to counting of splash drops. The surface must be maintained perpendicular to the path of the drops or elongated traces are produced. Since the terminal velocity of raindrops varies with the size of the drops, it is not possible to maintain perpendicularity for all drops if there is any wind. Despite these objections the filter paper method remains the most popular method for obtaining drop size measurements.

Two methods have been used which depend upon the transformation of the liquid water droplet to a semi-rigid body. Bentley[9] caught the drop in a layer of uncompacted flour. The resulting dough ball was dried, and sorted by mechanical sieves. The most widely accepted raindrop size spectra, obtained prior to World War II, were obtained by Laws and Parsons[10] using the dough pellet method. Laws and Parsons were interested in the problem of soil erosion and obtained their data to better estimate the kinetic energy and momentum transferred to the soil during a rainstorm. This data was used extensively for the early work in radar meteorology. Neuberger [11] suggested freezing the raindrop and measuring the resultant ice pellet. Both of these devices suffer from inability to sample large volumes for extended periods of time. Furthermore, Neuberger had difficulty with the drops fracturing and splintering during the freezing process.

Bowen[12] suggested the use of a horizontal wind tunnel to sort the raindrops into size classifications. The drops were allowed to fall into a moving air stream. The smaller

drops are transported further along the tunnel than the larger drops. A series of drop sensing devices are placed at the bottom of the air stream to determine the number of drops in each size class. This type of device does not work well if the drops have horizontal velocities on entering,,

A device has been constructed by Cooper[13] which responds to the momentum of the falling raindrop. A microphone can be coupled to a membrane and the membrane exposed to the rain. A drop hitting the membrane produces an electrical pulse from the microphone that can be measured and related to drop size. Several instrumental difficulties with these devices have been encountered. The sensitivity of the microphone varies with the location of drop impingement on the membrane. Because of dynamic range difficulties, several instruments are needed to cover the range of drop sizes encountered. Buffeting of the membrane by the wind creates a serious noise problem.

The amount of light scattered from individual raindrops can be used to measure the size of raindrops. This technique was first employed by Gucker[14] for very small particles. Mason[15] developed an instrument for measuring raindrop sizes. The drops were allowed to fall through a collimated, rectangular beam of light. The scattered light from about 20° off the axis was focused onto a phototube and the voltage pulse from the phototube measured. The sampling volume was optically defined. This device suffered from edge effects or loss of sensitivity when the drop approached or split one of

the optically defined edges. In addition the requirement that only one drop be in the sample volume at a time restricts the sample volume to be small. This device was improved upon by Dingle[16] who mounted the light source and the phototube on movable arms. These arms are then rotated around a vertical axis to increase the effective rate of volume sampling. The device has operated successfully, but still with smaller sample volumes than desired. The calibration of the device is difficult and does not remain stable due to arc lamp aging. Uneven background illumination has produced some difficulty.

Liquid drops have been photographed successfully in the laboratory for many years. As early as 1908 Worthington[17] photographed water drops falling into liquids. As a light source an electrical spark was used. Edgerton[18] photographed milk drops using a photoflash tube. Best[19] photographed raindrop-sized water drops in the laboratory to determine the free fall shape of the drops. Elliott[20], Kelly[21], and McCullough[22] developed cameras for photographing cloud droplets. These cloud droplet cameras sampled only a very small volume. Prior to the development of the Illinois raindrop camera no successful large field drop size camera has been reported. The prototype 12-inch system was reported by Jones,[23] Since a large volume of rain should be sampled frequently in a radar-rainfall study, Jones constructed a camera unit using a 12-inch mirror. After further analysis, it was found that a larger sample was desirable in a shorter

time period. A larger system was designed and used for this study.

A complete bibliography on raindrop sizing and counting devices prior to 1957 was compiled by Pearson and Martin.[24] This bibliography was prepared to evaluate automatic techniques for raindrop size measurement. At present there is no fully automatic means of obtaining large samples of rain and determining the spectra automatically.

SCATTERING THEORY

The basic radar equation which relates properties of the target and measurable radar parameters is

$$\frac{P_r}{P_T} = \frac{G^2(\theta,\phi)\lambda^2}{(4\pi)^3 r^4}\sigma \qquad (1)$$

where

P_r = the received power at the antenna terminals

P_T = transmitter power at the antenna terminals

$G(\theta,\phi)$ = the power gain of the antenna at azimuth angle θ and at elevation angle ϕ measured with respect to the axis of the antenna

λ = wavelength of the transmitted signal

r = distance to the target

σ = radar back scattering cross section.

The term of interest in this paper is σ as it is the only parameter related to the rainfall. The radar back scattering cross section can be defined as the area which intercepts that amount of power which if scattered isotropically would give an echo equal to that from the target. The problem of determining the back scattering cross section of a spherical object has received much attention throughout the years. A recent article by Logan[25] describes some of the early work in scattering from spheres. Apparently, some of the earliest work was performed by Clebsch[26] in 1861. His work has been overlooked by later workers. The most referenced work to

scattering from a sphere is that of Rayleigh,[27,28] Rayleigh solved the scattering for spheres small with respect to the wavelength. Mie[29] produced a complete theory for the scattering from spheres of any material in a non-absorbing medium. Mie's work has been restated by Stratton[30] and Kerr.[31] Using the notation of these later workers, the important cross sections for this work are

$$Q_T = \frac{\lambda^2}{2\pi}\left[-Re\sum_{n=1}^{\infty}(2n+1)(a_n + b_n)\right] \qquad (2)$$

$$\sigma = \frac{\lambda^2}{4\pi}\left|\sum_{n=1}^{\infty}(-1)^n(2n+1)(a_n - b_n)\right|^2 \qquad (3)$$

where

Q_t = total attenuation cross section

σ = back scattering cross section

λ = wavelength

a_n = coefficient of the nth magnetic mode

b_n = coefficient of the nth electric mode

The values for a_n are given by Stratton in terms of spherical Bessel Functions. Lowan[32] calculated values for Q for a sufficient range of water spheres at 3-cm wavelength.

The a and b coefficients can be expanded in ascending order of α. Marshall[33] computes these coefficients to be

$$a_1 = -\frac{j}{45}(m^2-1)\alpha^5$$

$$b_1 = -\frac{2j}{3}\frac{m^2-1}{m^2+2}\alpha^3\left(1+\frac{3}{5}\frac{m^2-2}{m^2+2}\alpha^2 - \frac{2j}{3}\frac{m^2-1}{m^2+2}\alpha^3\right) \quad (4)$$

$$b_2 = \frac{j}{15}\frac{m^2-1}{2m^2+3}\alpha^5$$

where

$$\alpha = \frac{\pi D}{\lambda} \quad (5)$$

D = diameter of the sphere

and m = complex index of refraction.

If $\alpha \ll 1$ only b_1 is important

and

$$Q_T = \frac{\lambda^2}{\pi}\alpha^3 \operatorname{Im}\left[-\frac{m^2-1}{m^2+2}\right] \quad (6)$$

$$\sigma = \frac{2\lambda^2}{3}\alpha^6\left|\frac{m^2-1}{m^2+2}\right|^2 \quad (7)$$

Equations (6) and (7) are of the form known as the Rayleigh formulas. The region within which these formulas are valid is known as the Rayleigh region. Kleinman[34] has suggested adoption of a definition of the Rayleigh region as that region in which the quantity of interest may be expanded in a convergent series in positive integral values of $k = \frac{2\pi}{\lambda}$ .A more restricted range for the Rayleigh region is used in meteorology where it is generally accepted as that region where the first term Is within 3 db of the exact value.

Haddock calculated values of the ratio of Qt (Mle)/Qt (Rayleigh) and were reported by Marshall.[33] These calculations

using water at l8°C and for 3-cm radar indicate that the estimate of Qt (Rayleigh) is different by a factor of 2 from Qt (Mie) when α - 0.15. This corresponds to a raindrop of diameter 1.4 mm which very commonly occurs. The calculations for Q_t in this report were performed using Lowan's Bureau of Standards Table.

Marshall also calculates the ratio of σ(Rayleigh)/ σ(Mie). For this ratio to be less than 2, the drop diameter must be less than 3 mm. A large percentage of the drops are smaller than 3 mm; however, the larger ones are the more important in terms of the radar scattering. At 10 cm the ratio of σ(Rayleigh)/ σ(Mie) is less than 1.1 for all raindrops up to 10 mm diameter. In this paper, the equations relating to back scattering cross sections are strictly valid only for 10 cm wavelength or longer and approximately valid for 3 cm wavelength. An evaluation has shown on limited amounts of data that for 3 cm wavelength an underestimate of σ of about 2 - 4 db could be made at the highest rainfall rates. Since most radars, to be used for quantitative measurement, are at wavelengths of 10 cm to avoid the attenuation problem, the need for correction by the Mie theory for this data does not seem desirable.

The equation for the back scattering cross section Is usually rewritten as

$$\sigma = \frac{2|K|^2}{3\lambda^4} D^6 \tag{8}$$

where

$$K = \frac{m^2 - 1}{m^2 + 2} \tag{9}$$

In the case of a radar observing a rainstorm, each of the raindrops returns power to the antenna. The contribution of each raindrop may be considered as a small voltage source of magnitude proportional to the square root of its back scattering cross section and of random phase. Lawson[35] and Uhlenbeck show that the average power expected from such an ensemble of scatterers is equal to the sum of the power scattered from each particle. In the case of a radar viewing a rainstorm, the total effective radar back scattering cross section, σ_T, is

$$\sigma_T = \frac{2|K|^2}{3\lambda^4} \sum_i D_i^6 \qquad (10)$$

where i ranges so that each raindrop within the entire radar volume is considered. Usually an assumption of the homogeniety of the rain is invoked which allows the following

$$\sigma_T = \frac{2|K|^2}{3\lambda^4} V \sum_1 D^6 \qquad (11)$$

where

V = the radar volume

and $\sum_1$ indicates that the summation should be performed over one cubic meter of air space. The quantity $\sum_1 D^6$ is defined as the radar reflectivity and is symbolized by Z. Some authors (Battan,[36] for instance) prefer $\sum_1 \sigma$ to be the radar reflectivity. Both definitions are in usage in meteorology. In this paper, radar reflectivity is defined as $Z = \sum_1 D^6$.

THE DROP CAMERA

After considerations of the other possible means for obtaining drop size spectra, the photographic method was chosen. The greatest advantage of this method is the possibility of obtaining relatively large sampling volumes. It was anticipated originally that at least one cubic meter of air space should be sampled. Later analysis has shown that in actuality an even larger sample would have been desirable. In addition, photographic methods yield high accuracy of measurement as well as giving some information on the shape of the raindrop.

General Design Criteria

In order to be a useful instrument, the camera must satisfy the following design criteria:

a. Capable of measurement of raindrops from 0.5 mm to 5.0 mm
b. Capable of obtaining a sample size of at least one cubic meter of air space per minute
C. System should not require film resolution of greater than 100 lines per millimeter
d. System to operate semi-automatically$_e$

Discussion of Criteria

The lower size limit on the measurable drop size was arbitrarily chosen at 0.5 mm. The necessity for measurement of smaller drops is quite low if the measurements are to be

used in radar rainfall work. The Rayleigh scattering theory indicates that it would require 64 times as many 0.5 mm drops as 1.0 mm drops to produce the same radar reflectivity. The upper limit was tentatively set at 5.0 mm since it was anticipated that larger drops did not occur in natural rainfall. This assumption was found later to be untrue.*

The choice of a one cubic meter sample was thought to be sufficiently large to yield a good estimate of rainfall rate and radar reflectivity. It was also a compromise with the amount of labor involved in reducing the data. Since each drop would require manual measurement from the film and since concentrations of the order of 1000 drops/m^3 are not uncommon, the use of larger volumes becomes impractical in that the data reduction becomes more formidable.

The system film resolution of 100 lines/mm was set as a criterion since it was found experimentally that this was achievable with modest care in film handling and development. Higher resolution required special film such as "micro-copy" which is very slow and since raindrops are moving at velocities up to 10 m/s, the slower film would not be usable.

The criterion that the system should operate semi-automatically meant that the camera was to be started by some form of rain switch and then operate automatically until one roll of film was expended.

---

*The largest all-liquid drop measured was 8.4 mm in diameter. Figure 8 illustrates the number of drops larger than 5.0 mm which occur.

All of these design criteria were met by the drop camera.

Optical Design

One of the first considerations in a photographic measuring device must be the effects of perspective. Perspective effect, if present in the final film, would mean that different magnifications would be necessary in interpreting the image measurements. One way of reducing the effects of perspective is to use a telecentric optical system. This system is illustrated In figure 1. The basic distinction In this system is that the aperture stop (that stop which delineates which of the light rays from the object pass through the system) is placed at the focal point of the first lens of the system. If the aperture stop were actually an Infinitesimal opening, all rays passing through the aperture and intercepting the first lens would be parallel in object space. Thus, In figure 1, the only light from an object A and an object B of equal size which would pass through the aperture would be the ray from A through B. Since these are all parallel rays, the effect of perspective is completely nullified.

In actuality, of course, it is not possible to have an infinitesimal hole, but even with a larger opening the same principle is applicable. Actually, the use of a very small hole introduces further difficulties in that diffraction effects become important prohibiting the formation of a good image. Furthermore, when film is placed behind the aperture stop with or without another lens, considerations of depth of

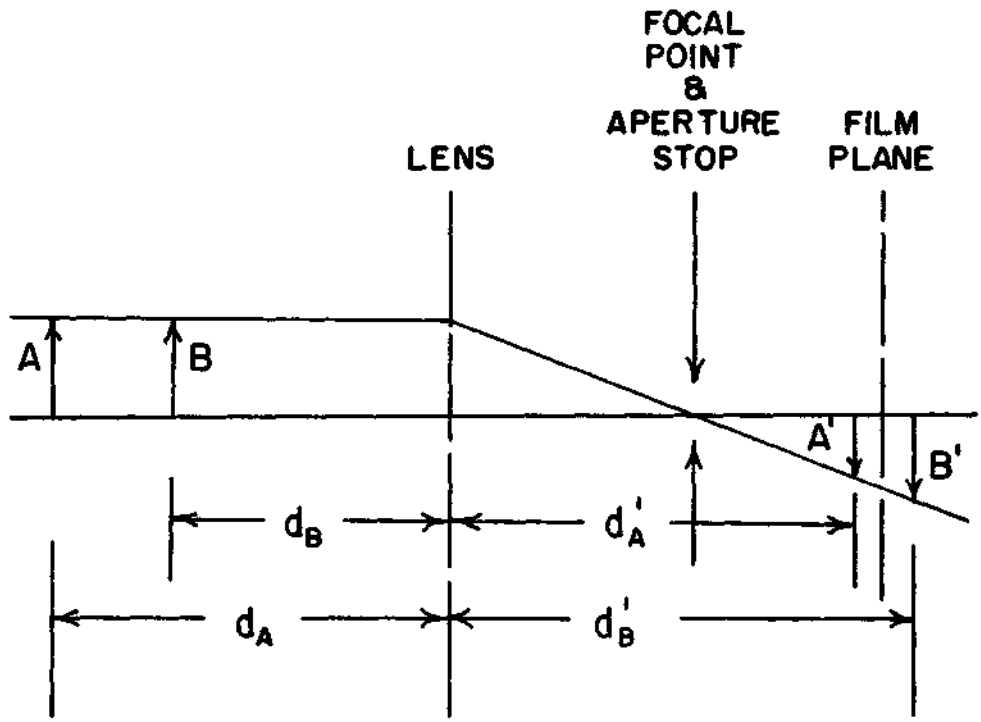

Fig. 1 OPTICAL DRAWING OF TELECENTRIC SYSTEM

field become important. With reference to figure 1, the angle of rays accepted by the aperture stop is different for objects at A than those at B. This can be seen by considering the thin lens formula

$$\frac{1}{d_A} + \frac{1}{d'_A} = \frac{1}{f} \qquad (12)$$

where

d_A = distance of the object A from lens

d'_A = distance of the image of A from lens

f = focal length of lens.

If $d_A > d_B$ then $d'_A < d'_B$ and the angle from the axis to the stop must be different as viewed from d'_A and d'_B. Since the rays are converging at different angles, any further lens system will not be able to simultaneously focus all points in object space.

One limitation of the telecentric optical system is that the physical size of the first lens of the system must be as large as the object space to be photographed. Initially, a 12-inch system using 35-mm film was used and after proving the general idea, three larger 30-inch mirror systems were obtained. Considerations are given only to the 30-inch system. A 30-inch size was chosen as a break point in the cost of mirrors. The overall object space can then be considered to be 30 inches in diameter. The desired resolution of 0.25 mm in object space requires that the film be capable of 3000 line resolution. Using 70-mm film, with a frame size of 56 mm, the film resolution has to be about 55 lines/mm.

Having chosen the film size as 70-mm film and a mirror size of 30 inches, the magnification of the optical system is obtainable by the ratio of these sizes. This yields a magnification of 0.075. The final optical layout is illustrated in figure 2. The first lens of the system is a mirror with a relatively long focal length,

A Newtonian telescope system was chosen to provide the maximum usable area of the mirror and still permit a large camera area. The diagonal flat introduces no difficulties in the design of the optical system and only a minor amount of additional field alignment is required.

Back lighting or shadow lighting was chosen as the most direct method of assuring uniform illumination throughout the entire sampling volume.

The magnification of such a system can be determined to be equal to the ratio of the focal length of the second lens to the focal length of the mirror. The focal length of the mirror was chosen as 4000 mm. Thus, with the desired magnification, a second lens of 300 mm focal length was obtained.

Consideration of the depth of field permissible and the aperture size required are now considered. The depth of field for a given defocusing or circle of confusion is given by Hardy and Perrin[37] as

$$D = \frac{z'\rho}{m\rho - z'} + \frac{z'\rho}{m\rho + z'} \tag{13}$$

where

D is the depth of field

z' is the radius of circle of confusion

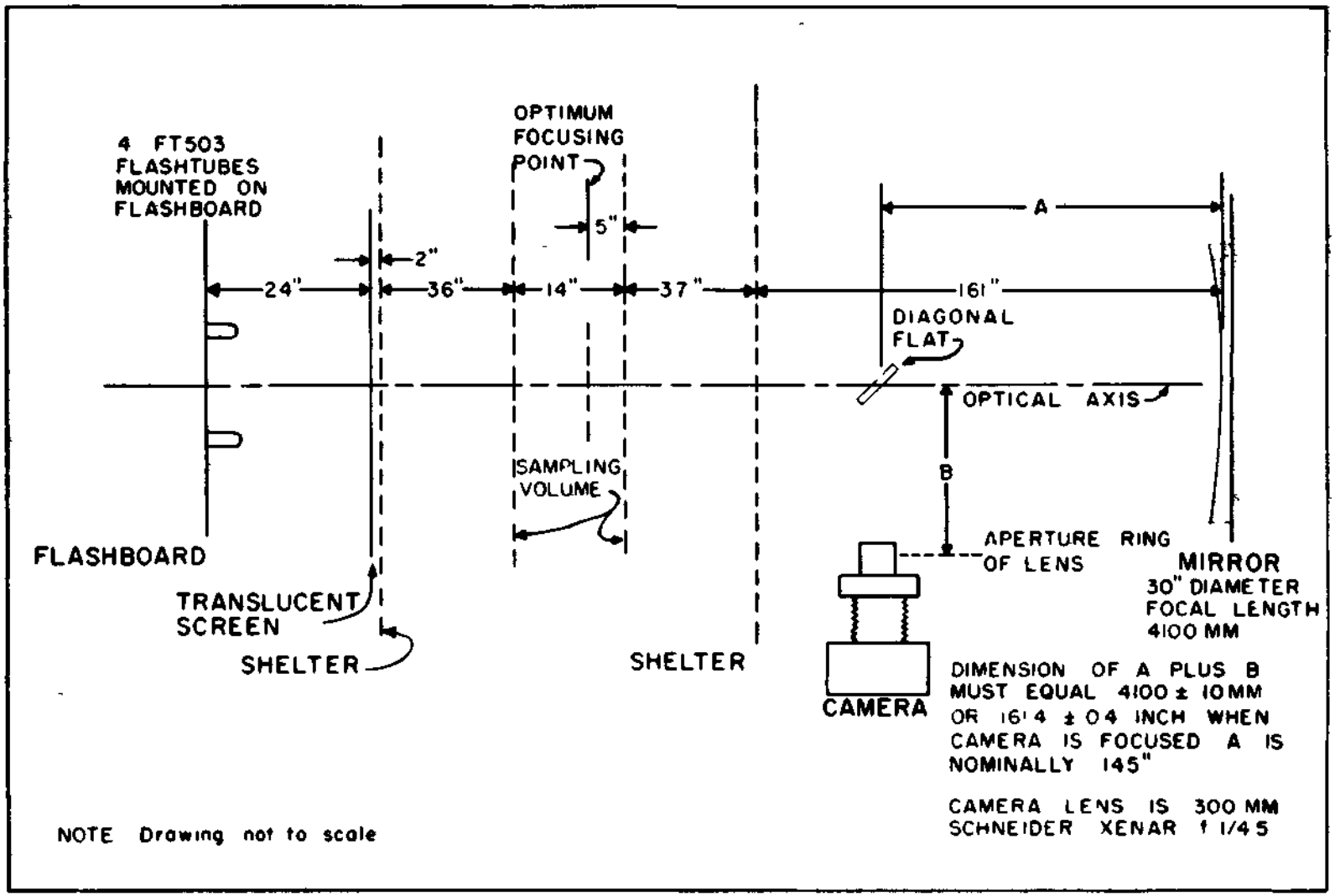

FIG.2 OPTICAL POSITIONING OF DROP CAMERA, TOP VIEW

m is the system magnification

ρ is the radius of entrance pupil

p is object distance referred to entrance pupil.

The symbolism used is the same as used by Hardy and Perrin and illustrated in figure 3.

As a first order approximation, the size of the circle of confusion is small with respect to the size of the exit pupil ($m\rho$) so that equation (13) becomes

$$D = \frac{2Z'\rho}{m\rho} \tag{14}$$

If the system is to be optimum, the radius of circle of confusion due to defocusing should be equal to the radius of circle of confusion due to diffraction effects around the aperture. This latter radius is given by Hardy and Perris as

$$Z' = \frac{0.61\lambda}{\tan\theta'} = \frac{0.61\lambda}{(\rho'/p')} \tag{15}$$

where

Z' = radius of circle of confusion

λ = wavelength of light

θ' = 1/2 angle of exit pupil as viewed from image point.

There is another relationship between the magnification of a system and the 1/2 angles of the entrance and exit pupils. This is

$$m = -\frac{\rho\rho'}{pp'} \tag{16}$$

Since values of entrance and exit pupils are not known, it is advantageous to eliminate these values from the equations if possible.

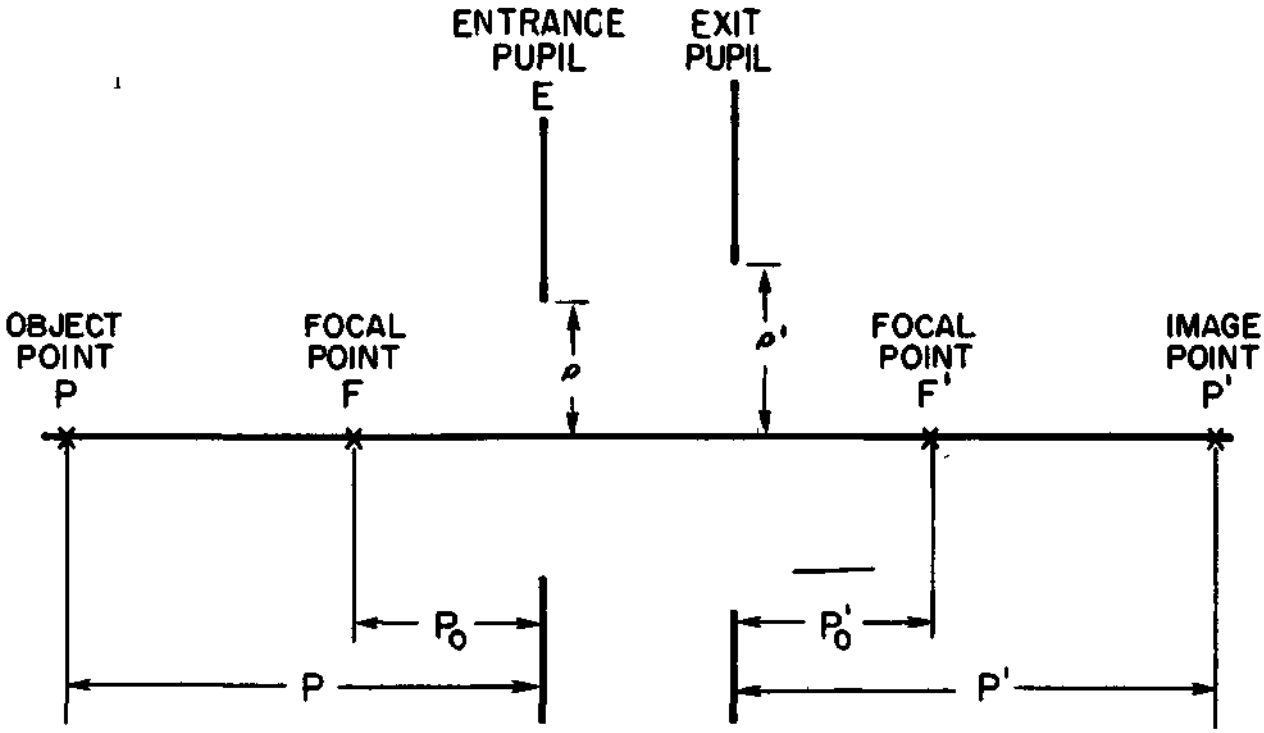

Fig. 3 GENERAL OPTICAL DRAWING

$$D = \frac{2Z'}{m\rho} = \frac{2Z'}{m}\left(-\frac{\rho'}{m\rho'}\right) = -\frac{2Z'}{m^2}\left(\frac{Z'}{0.61\lambda}\right)$$
$$= \frac{2Z'^2}{0.61\lambda m^2} = \frac{2Z^2}{0.61\lambda} \qquad (17)$$

where Z = the size of the radius of circle of confusion imaged back into object space.

Using a value of Z = 0.25 mm with λ - 5.10^{-4} mm yields a depth of field D = 410 mm $\simeq$ 16 inches.

Equation (17) gives a relationship between depth of field and radius of the circle of confusion in object space. In this equation there remains no variable related to any-particular optical system. Thus, it is apparent that for any optical system whatsoever, the depth of field cannot be any greater than allowed by equation (17).

Since the depth of field is fixed by optical necessity, the choice of a large diameter first mirror for the system is essential in order to have a large sample volume. The appropriate aperture may now be calculated by using equation (14).

$$\frac{\rho}{\rho} = \frac{2Z}{D} = 1.22 \cdot 10^{-3} \qquad (18)$$

This ratio multiplied by the distance of the object to the mirror yields the radius of the circle on the mirror which contributes to the image of a point in object space. The object distance of 4300 mm was chosen which yields a radius on the mirror of 5.25 mm. The virtual image by the mirror of an object point 4300 mm away is 57,300 mm. By proportional triangles, the radius of the cone at the focal point of the

mirror is determined to be 4.87 mm. The f/stop is defined as the ratio of the focal length of a lens to the diameter of the entrance pupil and therefore the f/stop must be 300/9.75 or f/30.

Sample Volume

As a first approximation, the sampling volume for each frame is represented by a right circular cylinder 30 inches in diameter and 14 inches deep. The depth of cylinder was reduced slightly to allow the raindrops to drift into the tunnels slightly and still be apparent on the negative. This yields a volume of 9900 cubic inches or 0.162 m^3. Thus, if a sample of 1 m^3 is desired, 7 frames are required. The cameras were operated with 7 exposures in 10.5 seconds. The camera film rewind time was 1.5 seconds and this is long enough to allow all raindrops to clear the sampling volume before a second picture is taken.

Light Source

Experience with the 12-inch camera led to the choice of 4 FT 503 flash tubes to provide the necessary illumination with the small f/stop required. Each FT 503 was operated from a 14 ufd condenser charged to 5000 volts producing an input energy of 175 joules for each tube. This energy is less than the rated value but larger condensers could not be used since the light duration had to be short. A large raindrop travels at about 10 m/s. If the travel is to be limited to less than the radius of the circle of confusion

in object space during flash time, less than 25 micro seconds duration must be achieved. The duration of the output light from the FT 503 with 14 μfd of capacity measured at one-half peak light was 10 micro seconds.

All four of the flash tubes were fired at the same time by use of a thyratron trigger circuit,, The total energy of 700 joules was sufficient to produce good exposure using Plus-X film in the camera. In fact a neutral density filter had to be used to prevent overexposure and resulting "wash out" of smaller drops.

General Camera Results

Figure 4 shows the finished camera installation. A number of tests were run to verify the design and construction of the camera. In one test, glass beads of known size were suspended from threads at different locations within the field of the camera. Throughout the entire 16 inches, no change in the size of the image on the film could be detected. There was of course better and sharper definition in the central area and progressively more fuzzy images as the beads were moved towards the extremes. In the central area an accuracy of ±0.05 mm could be achieved. This accuracy degraded to ±.2 in the vicinity of the near and far edges of the sampling volume. Astigmatism was apparent near the edges of the sampling volume which also degraded the accuracy of measurement in one of the dimensions. Beads as small as 0.3 mm in diameter could be recognized in the central area

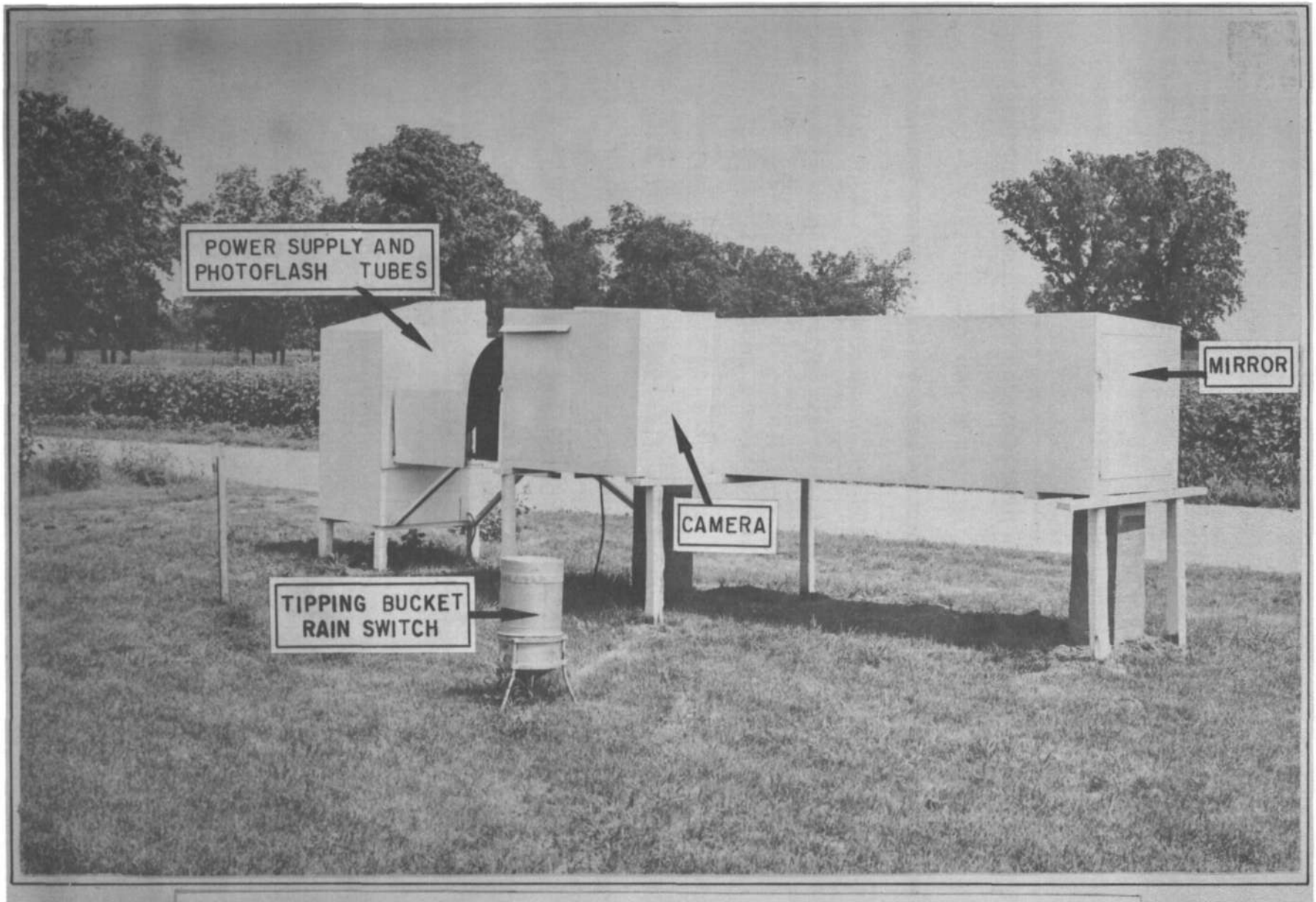

Fig. 4 EAST CENTRAL ILLINOIS DROP CAMERA INSTALLATION

but were not visible near the edges of the sampling volume,, A National Bureau of Standards optical resolution chart was obtained and was used for focusing and routine measurements of the resolution and the depth of field. Using this card, an overall resolution of over 2 lines per mm referred to object space was achieved over the entire sampling volume, routinely. Figure 5 shows an enlarged picture of raindrops obtained with the camera. The final enlargement here brings the raindrops to about twice life size. Figure 6 shows the entire frame from which figure 5 was obtained. This frame was obtained on July 25, 1964 in Illinois. The rainfall rate was 166 mm/hr. On this frame, there were 943 raindrops. Only the larger drops can be seen on the reproduction. This represents a concentration of 6600 drops/m^3. The radar reflectivity was $4.7.10^5 mm^6/m^3$ and the liquid water content was 7.38 g/m^3.

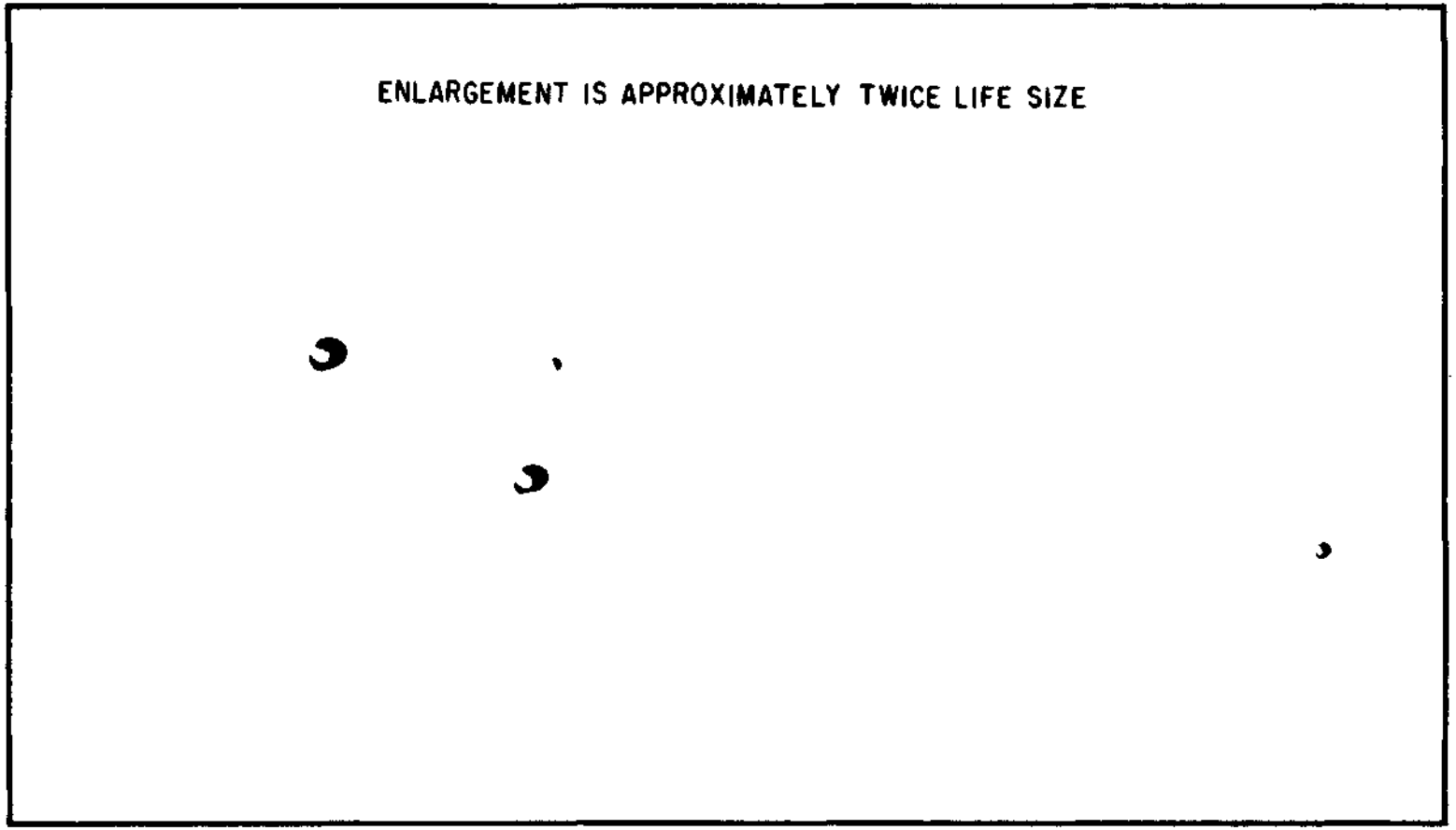

Fig. 5 PARTIAL FRAME OF ENLARGED RAINDROPS

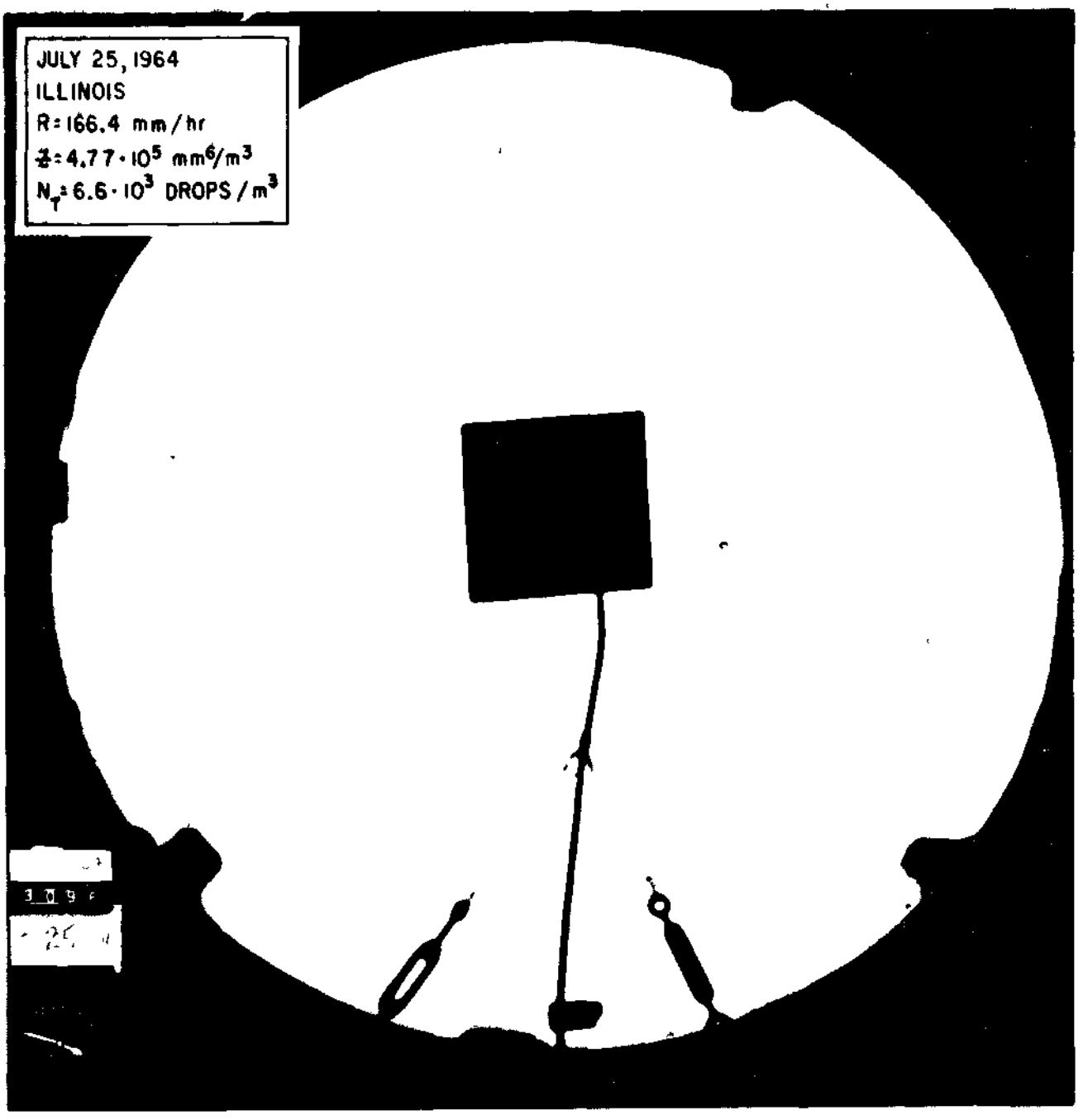

Fig. 6 EXAMPLE OF ONE FRAME OF CAMERA DATA

DATA COLLECTION AND MEASUREMENT

Locations

After a limited amount of raindrop camera data was obtained in Illinois, the cameras were sent to seven locations. The intent was to sample rainfall at different climatic areas to determine the differences in the radar-rainfall rate relationship. The seven locations chosen were: 1) Miami, Florida; 2) Corvallis, Oregon; 3) Majuro, Marshall Islands; 4) Bogor, Indonesia; 5) Woody Island, Alaska; 6) Island Beach, New Jersey; 7) Franklin, North Carolina. These seven locations represented nearly all of the non-arid major climatic regimes on the earth. The cameras were operated at these locations by sub-contract with the University of Miami, Oregon State College, University of Indonesia and with the United States Forest Service in North Carolina. Local Weather Bureau employees operated the camera in the Majuro Islands, and Federal Aviation Agency employees operated the camera in Alaska. The camera in New Jersey was originally to have been operated by personnel from Fort Monmouth, but most of the operation was performed by a local high school teacher.

Table 1 shows the locations where data have been obtained along with the distribution of data within the year. Most of the locations have data throughout the year. The Oregon installation was operating through the summer months but the

TABLE 1

DISTRIBUTION OF DATA COLLECTION BY MONTHS

Location	Jan	Feb	Mar	Apr	May	June	July	Aug	Sept	Oct	Nov	Dec	Total
Woody Island, Alaska	6	5	3	6	9	8	7	10	5	3	10	2	74 Days
	225	133	33	216	351	442	343	391	56	94	326	78	2688 Samples
Miami, Florida	7	1	9	4		3	8	12	9	6	6	7	79 Days
	394	66	306	46	448	82	207	250	128	189	184	206	2506 Samples
Majuro, Marshall Islands	4	1	7	20	11	12	7	11	7	4	5	6	95 Days
	81	44	67	445	215	524	271	457	208	96	63	81	2552 Samples
Corvallis, Oregon	12	1	10	16	-	9	-	-	-	-	-	11	59 Days
	501	8	198	358	-	203	-	-	-	-	-	435	1703 Samples
Bogor, Indonesia	14	4	15	13	5	1	-	-	-	-	12	12	76 Days
	426	55	333	253	63	16	-	-	-	-	239	494	1879 Samples
Champaign, Illinois	1	-	1	1	4	2	6	13	3	5	-	-	36 Days
	17	-	20	14	68	41	208	343	152	256	-	-	1119 Samples
Island Beach, New Jersey	6	9	6	7	5	13	9	7	5	8	8	4	87 Days
	199	501	236	298	121	486	292	122	92	287	326	187	3147 Samples
Coweeta, North Carolina	6	10	17	9	7	14	15	11		4	7	8	115 Days
	357	532	674	410	283	661	553	384	198	123	213	416	4804 Samples
										Totals			621 Days
													20,398 Samples

climate is such that no rain falls in the summer. The Indonesian system was the poorest sample. Rain does occur through the summer months but no sampling was obtained. In table 1 "sample" refers to a one-minute sample of a rainfall for which a non-zero rainfall rate was computed.

Photographic Measurements

After exposure, the film was processed in a tank under controlled temperatures to provide a fine grain negative. The development was in a diluted solution of D-76 with a development time of twice normal. The film was projected with a magnification such that the projected images were twice life size. At first the images were measured using a calipers and the values manually read and tabulated. Using this procedure, one minute of data required about 4 hours to measure and it became apparent that a more efficient means was needed.

A semi-automatic system was designed which permitted automatic reading of the calipers and entering of the results into an IBM machine. A caliper was fabricated in such a way that a lead screw moved one of the jaws of the caliper. Coupled to the lead screw was a ten position switch. Also coupled to the lead screw by a Geneva gear was a second ten position switch. The lead screw was made with 5 threads per centi-meter so that one complete turn produced a movement of the measurement jaws of 2 mm. Since the directly coupled switch had ten positions, each switch position represented 0.2 mm

movement of the jaws. Since an overall film magnification of 2 was employed, each switch position represented 0.1 mm of size of the original raindrop. This switch was then called the tenths switch. The second switch moved one position for each full rotation of the lead screw which was 2 mm movement of the jaws. With the magnification of 2, this switch represented the units of millimeters of the raindrop. A control box was designed and built which sequentially sampled the units switch and the tenths switch and transferred the information to an IBM 0-24 card punch.

The projection table was constructed with a glass area in the central part. Underneath the table and at an angle was a front surfaced mirror. A projector was mounted to the right of the table and projected forward into a mirror and then back into the mirror below the table and then upward onto a translucent screen. For convenience, the projector could be swiveled around both a vertical axis and a horizontal axis permitting the operator to bring all parts of projected images within easy reach of the front of the table. A photograph of the projection table, projector and control box is shown in figure 7. Using this system, the average time required to measure a one-minute data sample was reduced to about 1 hour. A horizontal and a vertical measurement was made of each raindrop. The assumption of an axis of vertical symmetry was made. This assumption is very nearly correct according to Jones.[38] Jones used the 12-inch prototype camera plus a second camera viewing the same drops at right

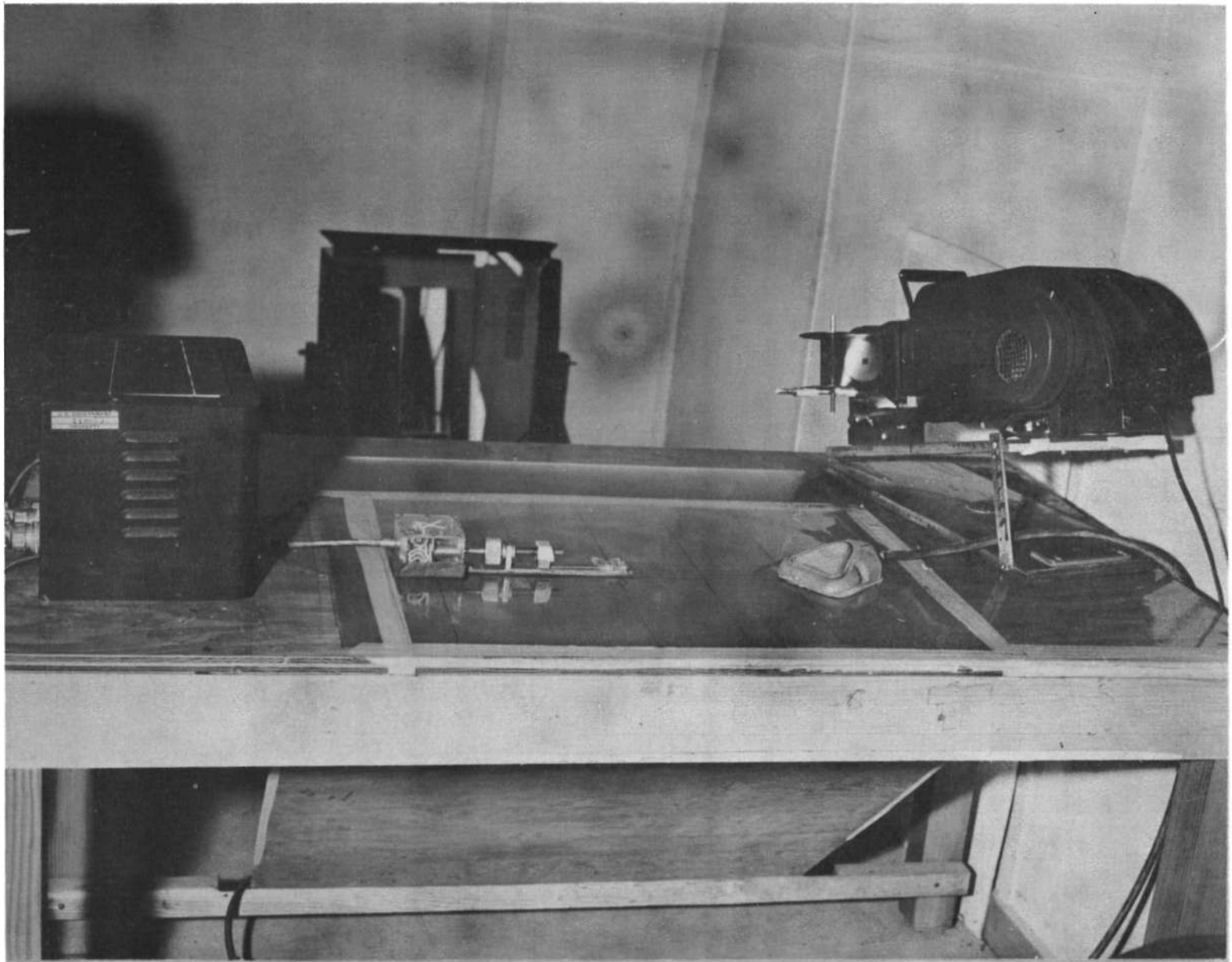

Fig. 7 PROJECTION TABLE AND CALIPERS

angles to determine whether the vertical axis was an axis of symmetry.

In considering the overall accuracy of the data, the measurement accuracy is the step which introduces the greatest uncertainty in the results. The task of measuring the raindrops individually is one that is quite boring; therefore, operators tend to become fatigued and careless, and this produces inaccuracies in the measurements. This is indicated by measurements repeated on an individual minute sample. In general, agreement of the number in each class to within ±10 percent can be achieved easily on the drops 0.8 mm and larger. The number of drops with diameters between 0.5 and 0.8 mm are frequently in greater error. The number of drops in these small sizes does not influence the radar back scatter cross section. At the same time, but to a lesser degree, the small drops do not influence the rainfall rate or the attenuation cross section as much as do the larger drops. The measurement accuracy for each drop is assumed to be ±0.2 mm as indicated by the resolution of the optics of the camera, the resolution of the film, and the resetability of the calipers to the drop size image. Under some conditions, it Is felt that the measurement accuracy may be better than ±0.1 mm.

Occasionally, some measurements have been made under conditions which prohibit this accuracy. In particular, some measurements of drop camera film that were obtained under interesting synoptic conditions were made even though

the glass on the shelters had become wet and caused some image blurring. The greatest danger in measuring under such conditions is that the blurring increases the possibility of missing the drop, especially a small one, completely.

Occasionally, because of a fault in the camera, a sample is composed of less than 7 frames. In this case, if there are 6 frames which are measurable, measurements are made on the 6 and the results are extrapolated to one cubic-meter sample. All drop size measurements that have less than 8 drops/m^3 have been discarded on the grounds that the sample is not representative and that the rainfall rate is too low to be of any significance in total amount.

Initial Drop Size Spectra

The IBM cards from the measurements were then submitted to a computer for determination of the equivalent spherical diameter and for tabulating into a frequency table. The equivalent spherical diameter should be calculated by taking the cube root of the product of the vertical measurement and the square of the horizontal measurement. It was noted, however, that if only 2 place accuracy was required, the simpler scheme of averaging the two readings and rounding downward provided a much faster and sufficiently accurate method. The tabulated drop size frequency spectra were punched on two IBM cards. These cards, called distribution cards, contained the number of drops in each 0.1 mm diameter interval from 0.5 mm to 7.9 mm. These cards served as data cards for the remainder of the computations.

The number of drops that can be measured in a one-minute sample has varied from the base of 8 drops/m^3 to a maximum of 13,000 drops per cubic meter.

The one-minute sample which produced the 13,000 drops is shown in figure 8. This minute was unusual, not only in the number of drops, but also in the low reflectivity for the rainfall rate. This indicates a loading of drops into the smaller size classes.

Initial Drop Computations

After distribution cards have been obtained, they are resubmitted to the computer. The computer then calculates the rainfall rate, R; the radar reflectivity, Z; the radar attenuation cross section, Q_t; and the liquid water content, L. This part of the computation amounts to solving the matrix equation

$$\begin{bmatrix} R \\ Z \\ L \\ Q_t \end{bmatrix} = \begin{bmatrix} R_{.5} & R_{.6} & R_{.7} \cdots R_{7.9} \\ Z_{.5} & Z_{.6} & Z_{.7} \cdots Z_{7.9} \\ L_{.5} & L_{.6} & L_{.7} \cdots L_{7.9} \\ Q_{.5} & Q_{.6} & Q_{.7} \cdots Q_{7.9} \end{bmatrix} \begin{bmatrix} N_{.5} \\ N_{.6} \\ N_{.7} \\ N_{7.9} \end{bmatrix} \qquad (19)$$

These constants have been determined by calculation. The rainfall rate constants are determined by application of the equation

$$R_D = \frac{\pi}{6} D^3 V_D \qquad (20)$$

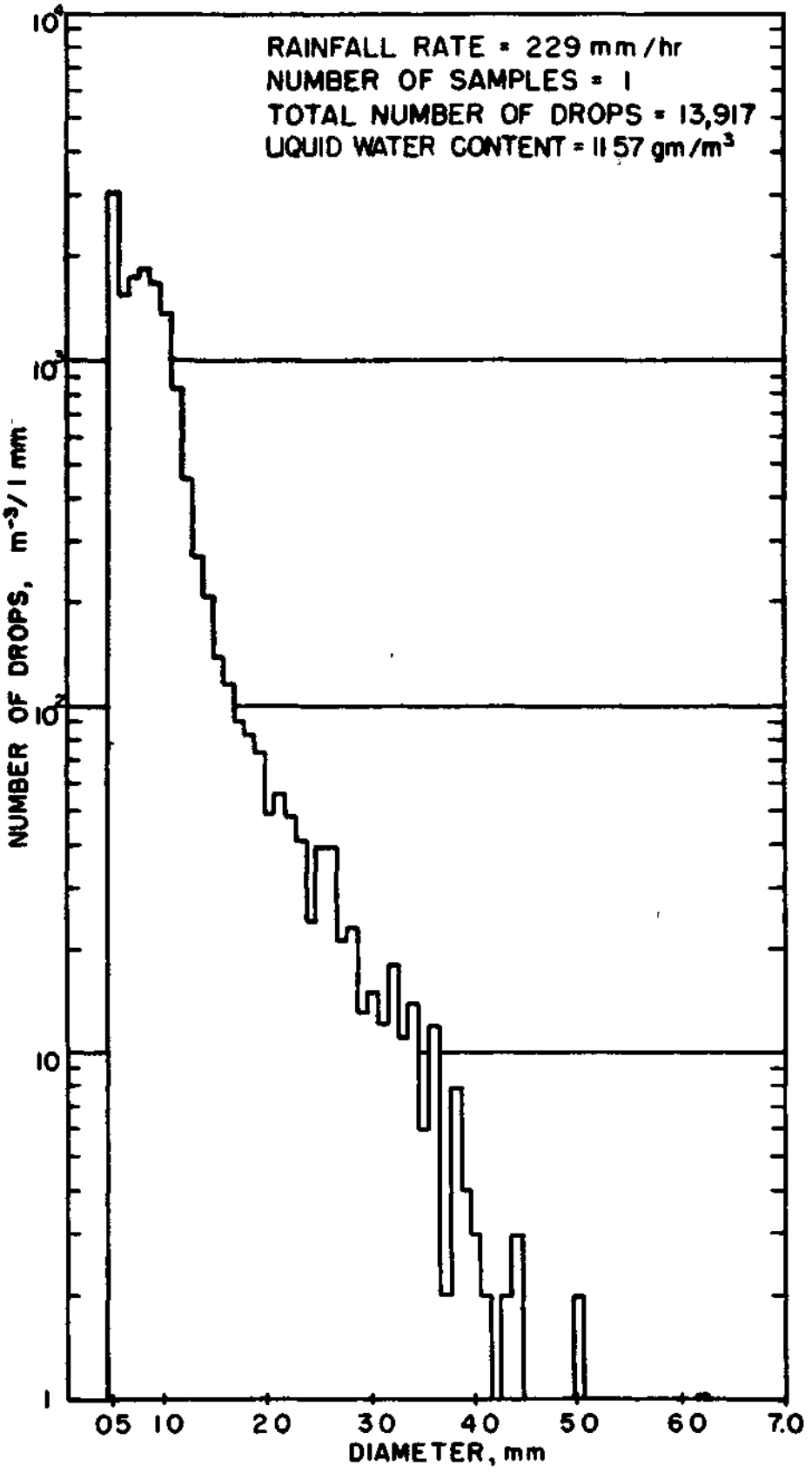

Fig 8 ONE-MINUTE SAMPLE OF LARGEST TOTAL NUMBER OF DROPS AT MIAMI, 1105 EST, JUNE 21,1958

This equation is solved at the end points of each interval. For example, a value is determined for a drop of 1.45 mm and for a drop of 1.55 mm. The results of these two extremes are averaged to determine the coefficient which is applied to the 1.5 mm drop. The fall velocity used in equation (20) is the terminal velocity of the drop as reported by Gunn and Kinzer.[39]

The values for Z, the radar reflectivity, are taken as the ΣD^6 over unit volume. Again, values for Z were calculated at the intermediate position between intervals and the two ends averaged arithmetically to determine the coefficient of each of the drop sizes. The units of the reflectivity, Z, are in mm^6/m^3.

The attenuation cross section has been calculated from the Mie scattering equations for 3-cm radiation. The same procedure for determining the constant for each of the class intervals is followed for this coefficient.

The constants of liquid water content are determined by the equation

$$L_D = \frac{\pi}{6} D^3 \qquad (21)$$

After the matrix multiplication is performed, another multiplication of each of the terms of the resultant matrix is multiplied by a term called the volume correction. For each drop camera location, the exact size of the volume of air sampled in 7 frames is determined by measurement of the distance between the shields and the amount of blocking due

to the optical components such as the diagonal flat and the mirror supports. After having determined the actual sampling volume, a correction is applied which produces the number of drops and the value of the variables as if one cubic meter were sampled. The size of the volume correction normally ranges between 0.97 and 1.1.

The values of these variables are then read from the computer and are combined with the observations made by the camera operator and with synoptic types determined by analysis of the conditions prevailing when the data was obtained.

AVERAGE DROP SIZE SPECTRA

Individual one-minute drop size distributions frequently exhibit large changes in the number of drops in adjacent classes. These fluctuations are attributed to statistical sampling noise and are related to the sample size. To reduce these fluctuations, a number of one-minute distributions representing the same rate were averaged. The resultant distributions are smoother and more easily classified. The averaging takes place by averaging the numbers of drops in each class interval.

Average distributions for different rainfall rates are exhibited in figures 9 through 16. The number of one-minute samples added together for each average is the number N_s shown in each figure. The average distributions are generally monomodal curves with modes occurring between 0.9 and 2 mm. Above the mode, the curves are very nearly straight lines on the semi-logarithmic plots. The number of drops decreases sharply for diameters less than the mode. The distributions are generally smoother and have a more systematic relation to rainfall rate at the low rates; at high rates, they are more erratic due to the smaller number of samples in the averages.

From these figures, some geographical variations can be noticed. The New Jersey curves have some similarity to those of Ma juro in the larger drop sizes. However, New Jersey rains have more total drops/m^3 than does Ma juro rain. The

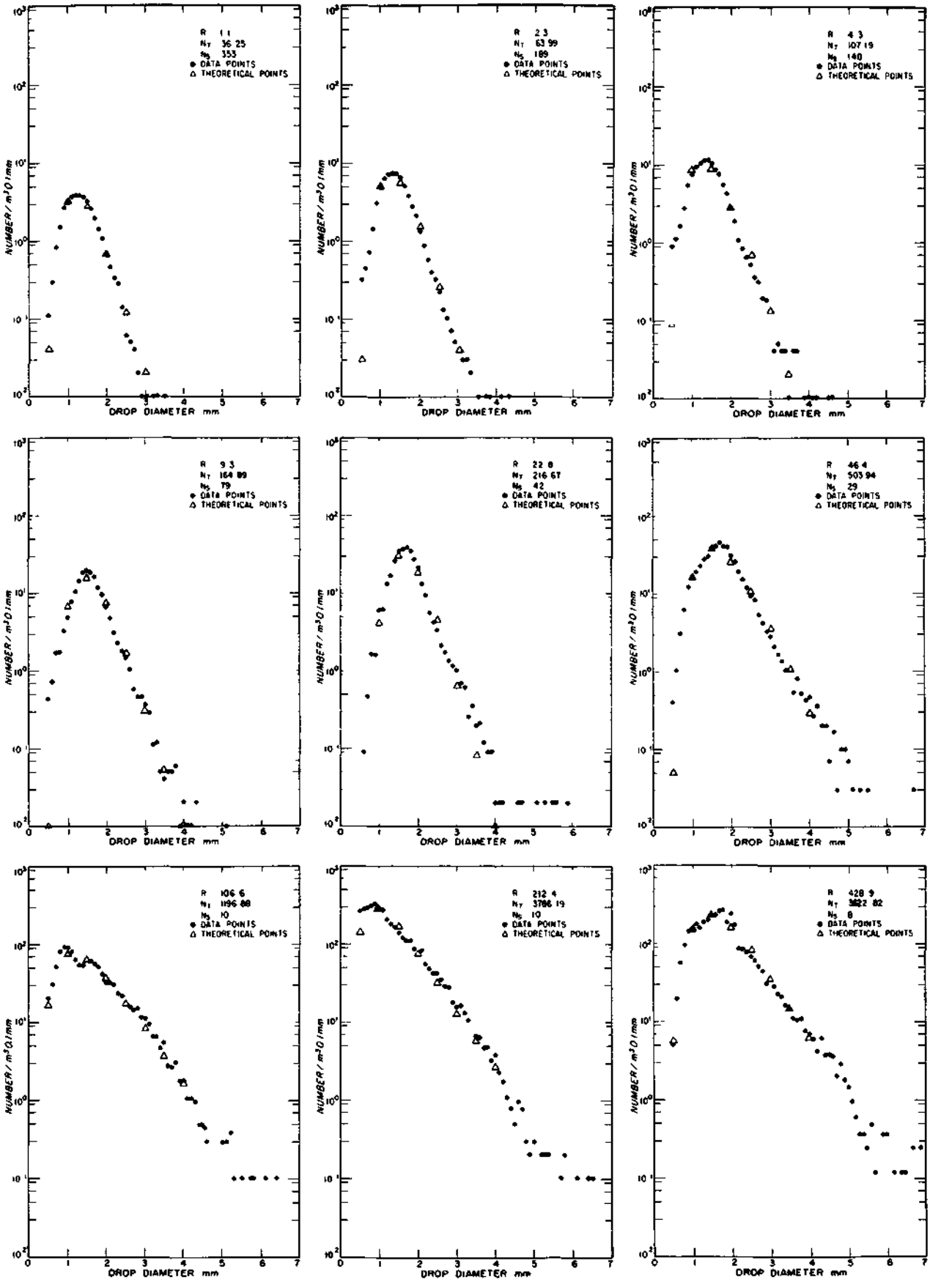

FIG. 9 AVERAGE DISTRIBUTIONS FOR ALL MIAMI, FLORIDA DATA

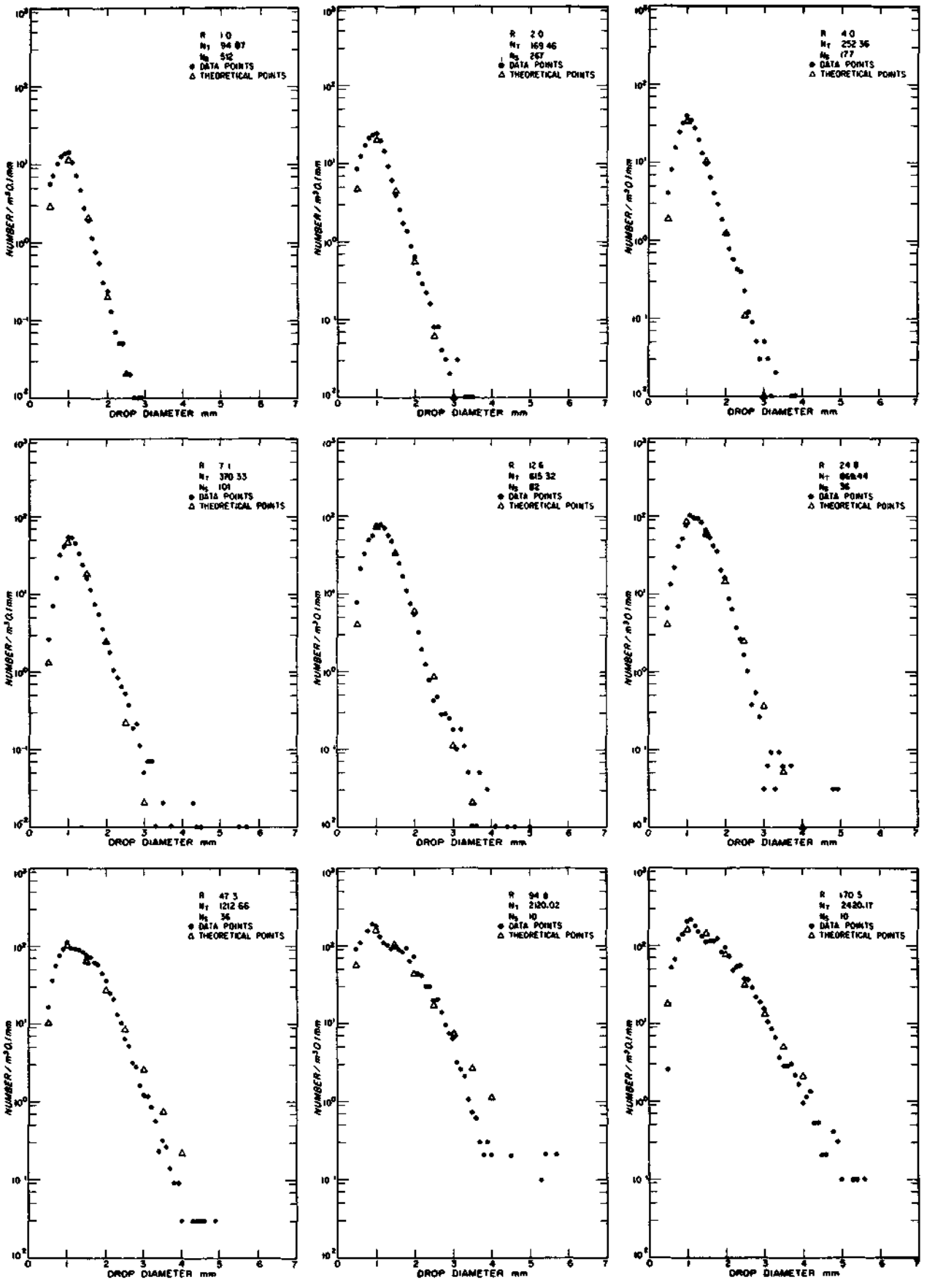

FIG 10 AVERAGE DISTRIBUTIONS FOR MAJURO, MARSHALL ISLANDS

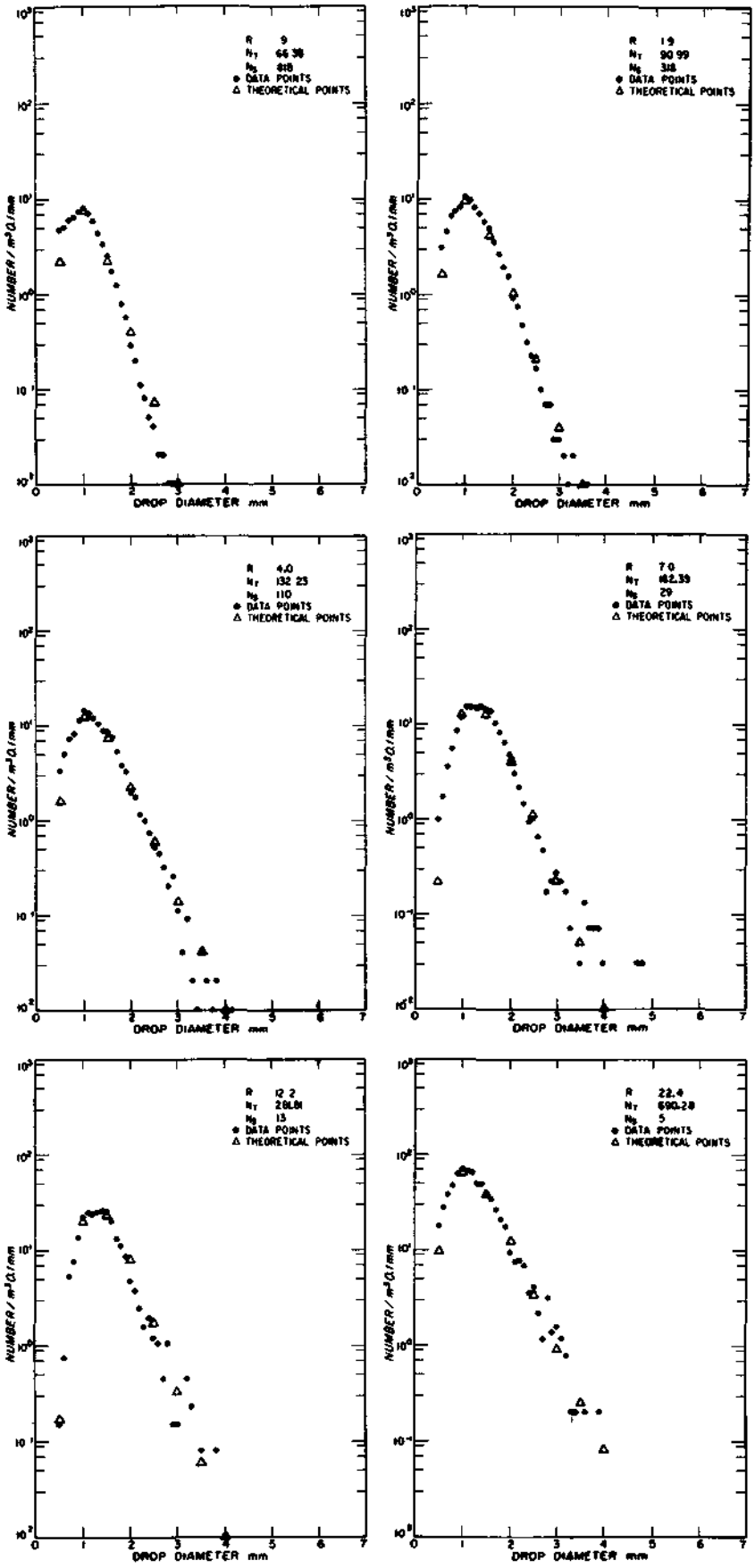

FIG II AVERAGE DISTRIBUTIONS FOR CORVALLIS, OREGON

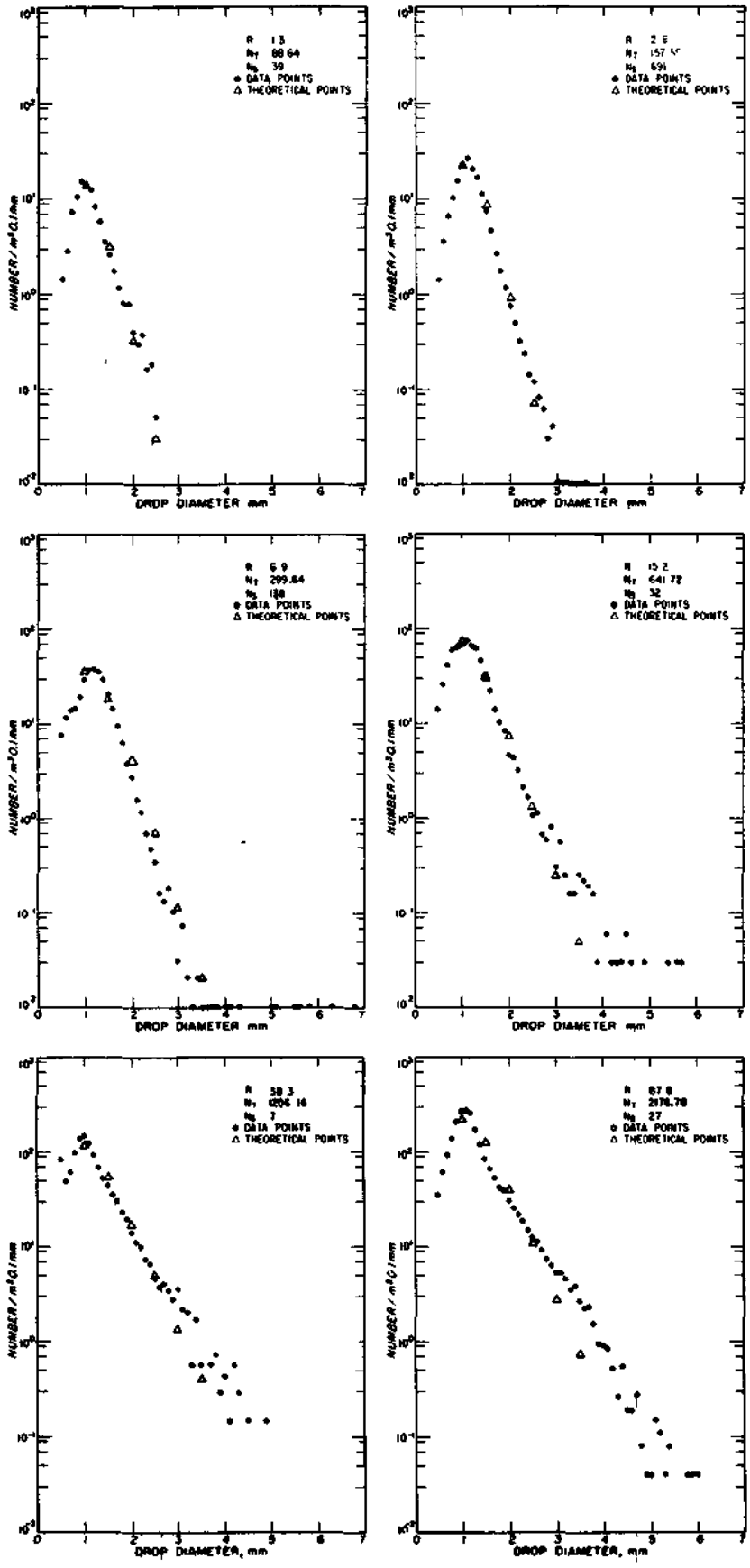

FIG 12 AVERAGE DISTRIBUTIONS FOR ISLAND BEACH. NEW JERSEY

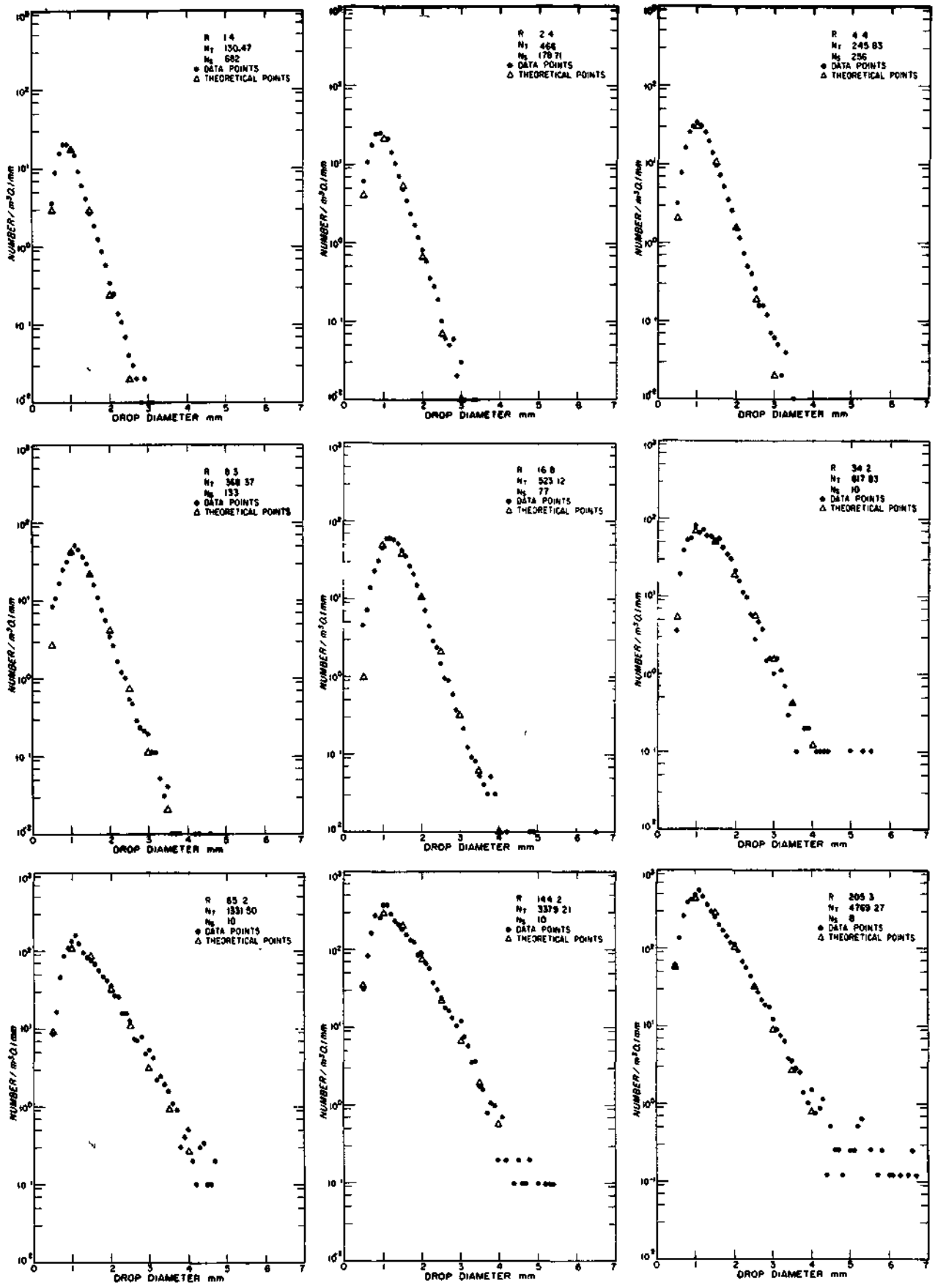

FIG. 13 AVERAGE DISTRIBUTIONS FOR COWEETA LAB., N. CAROLINA

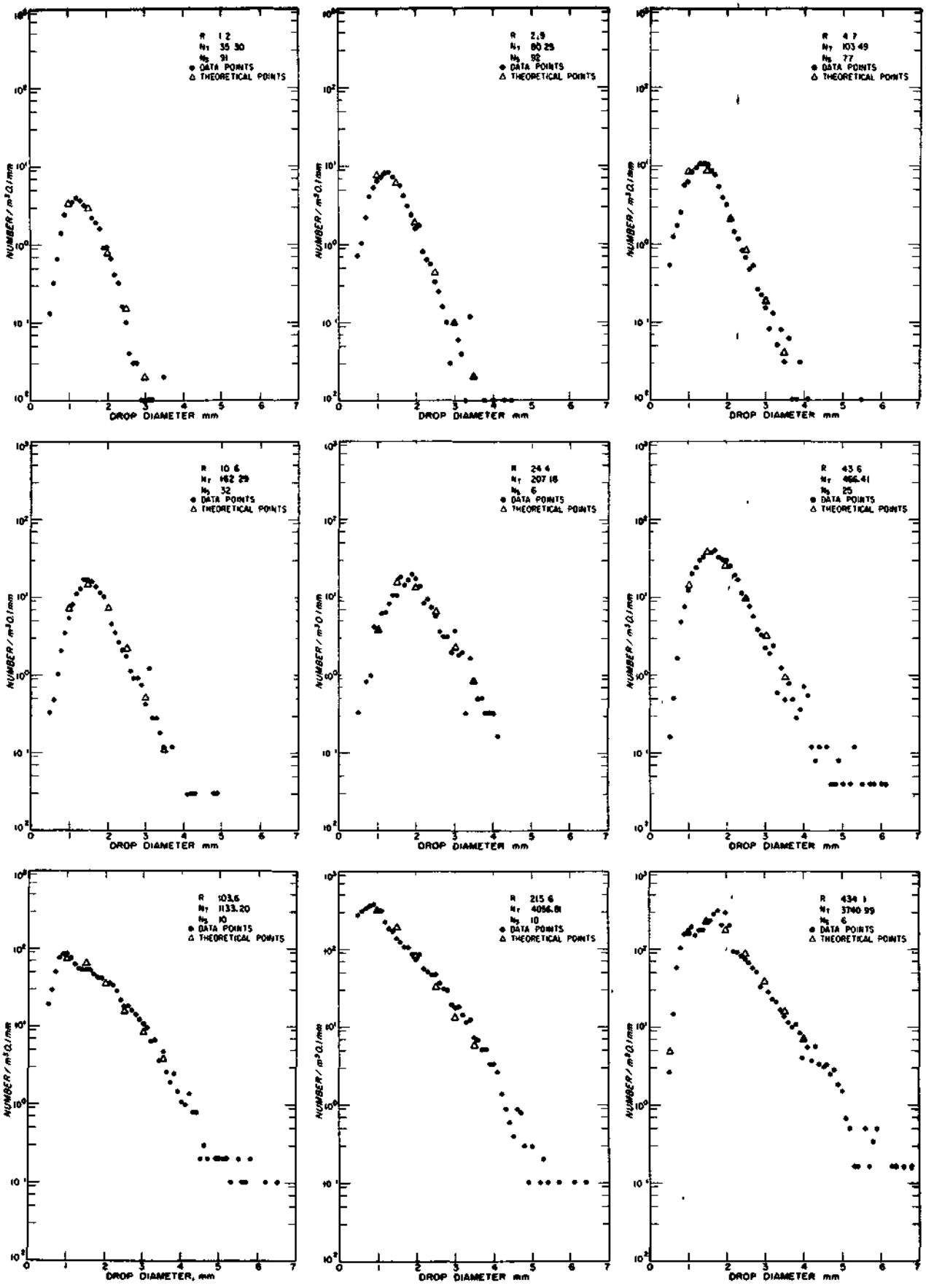

FIG 14 AVERAGE DISTRIBUTIONS FOR THUNDERSTORMS AT MIAMI, FLORIDA

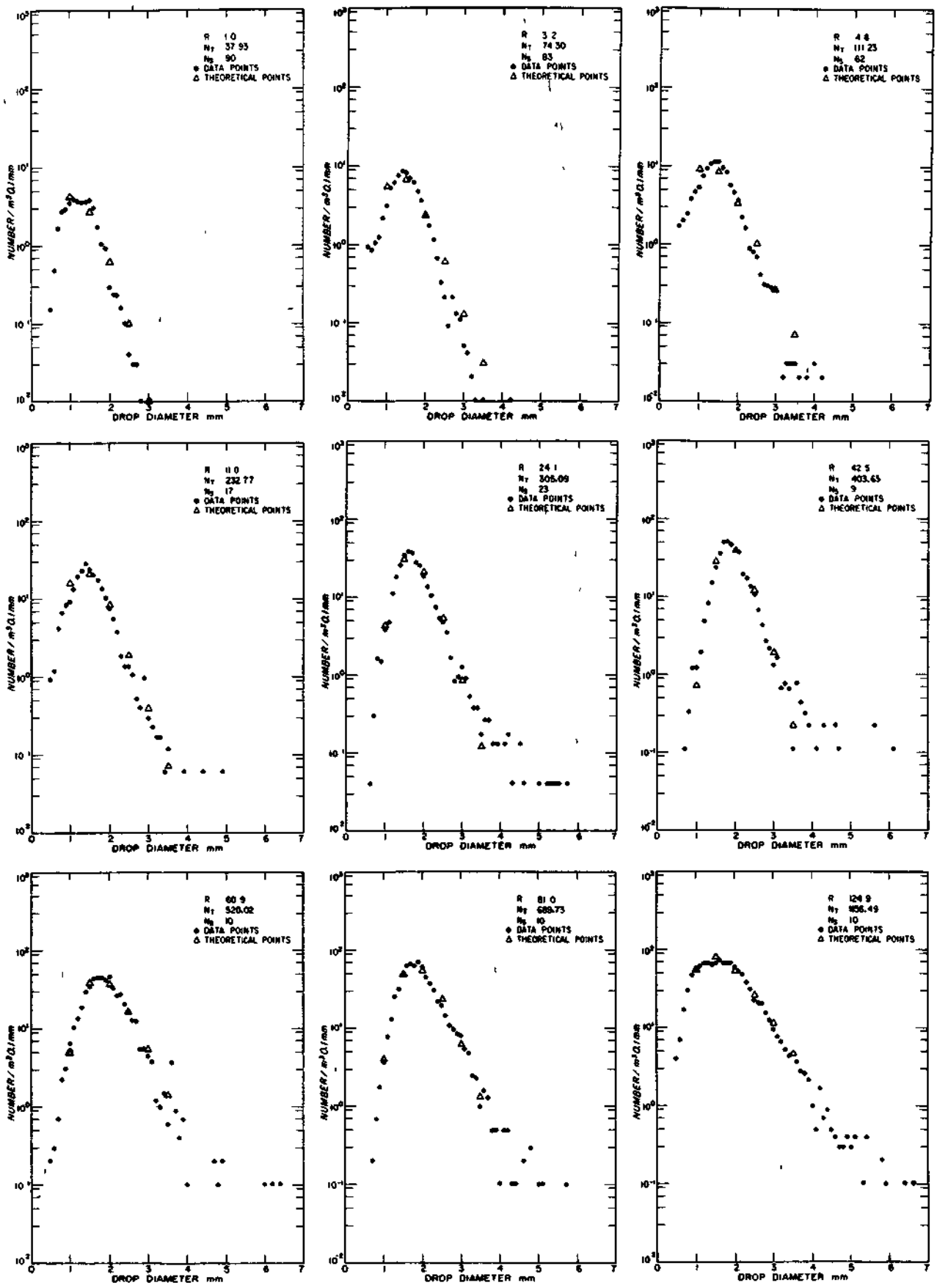

FIG. 15 AVERAGE DISTRIBUTIONS FOR RAINSHOWERS AT MIAMI, FLORIDA

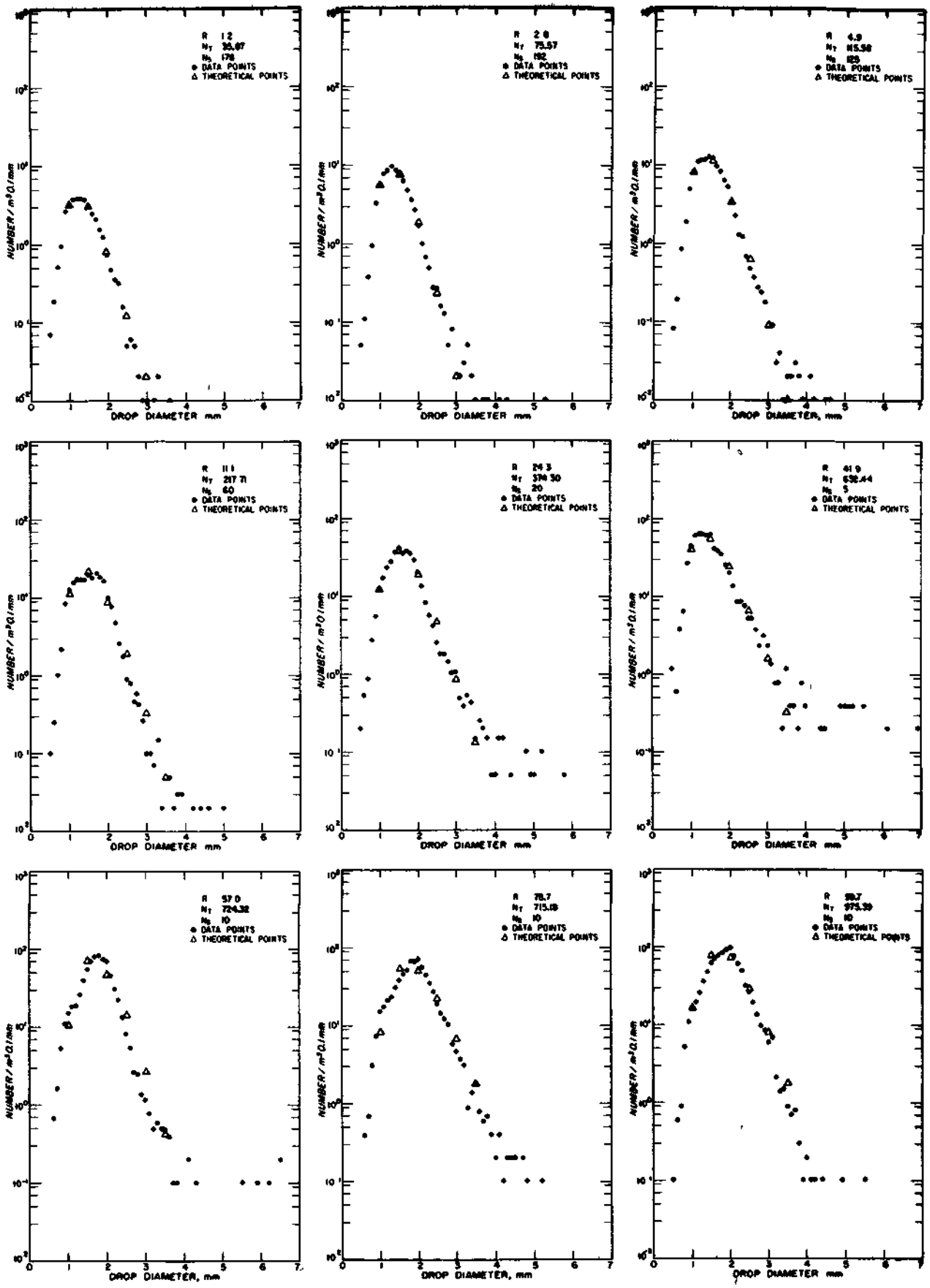

FIG 16 AVERAGE DISTRIBUTIONS FOR CONTINUOUS RAIN AT MIAMI. FLORIDA

Miami distributions are generally similar to those from New Jersey at large drop sizes, but have broader modes located at larger drop sizes. The Oregon data has only low rates since these are all that occurred. The Oregon data has broader modes for the same rates than those at any other location.

The average distributions for thunderstorms, rainshowers, and for continuous rain at Miami, Florida, are presented in figures 14, 15, and 16. An interesting feature of the thunderstorm curves, figure 14, is the rapid increase in small drops at rates above about 50 mm/hr. It should be noted, for example, that the number of 0.7 mm drops increases from 1.7 at 43.6 mm/hr to 335 at 215.6 mm/hr. For the same change in rate, the number of 3 mm drops increases from 2.2 to only 18. This effect is also apparent on the curves for all Miami data, figure 9, since at the high rates most of the rain came in thunderstorms.

In figure 17, average total number of drops, N_T, is plotted against the rainfall rate. The slope of the data for Miami increases beginning at 50 mm/hr. This is a result of the large increases of small drops. One explanation of this increase in small drop numbers may be raindrop break up. If this is the explanation, it should be reflected in a discontinuity of the number of large drops. Such a discontinuity has not been found, A more probable source of the large increase in numbers of small drops in high rates may be splash of raindrops from the tunnels and shelters of the raindrop camera. Even with these large numbers of small drops, the

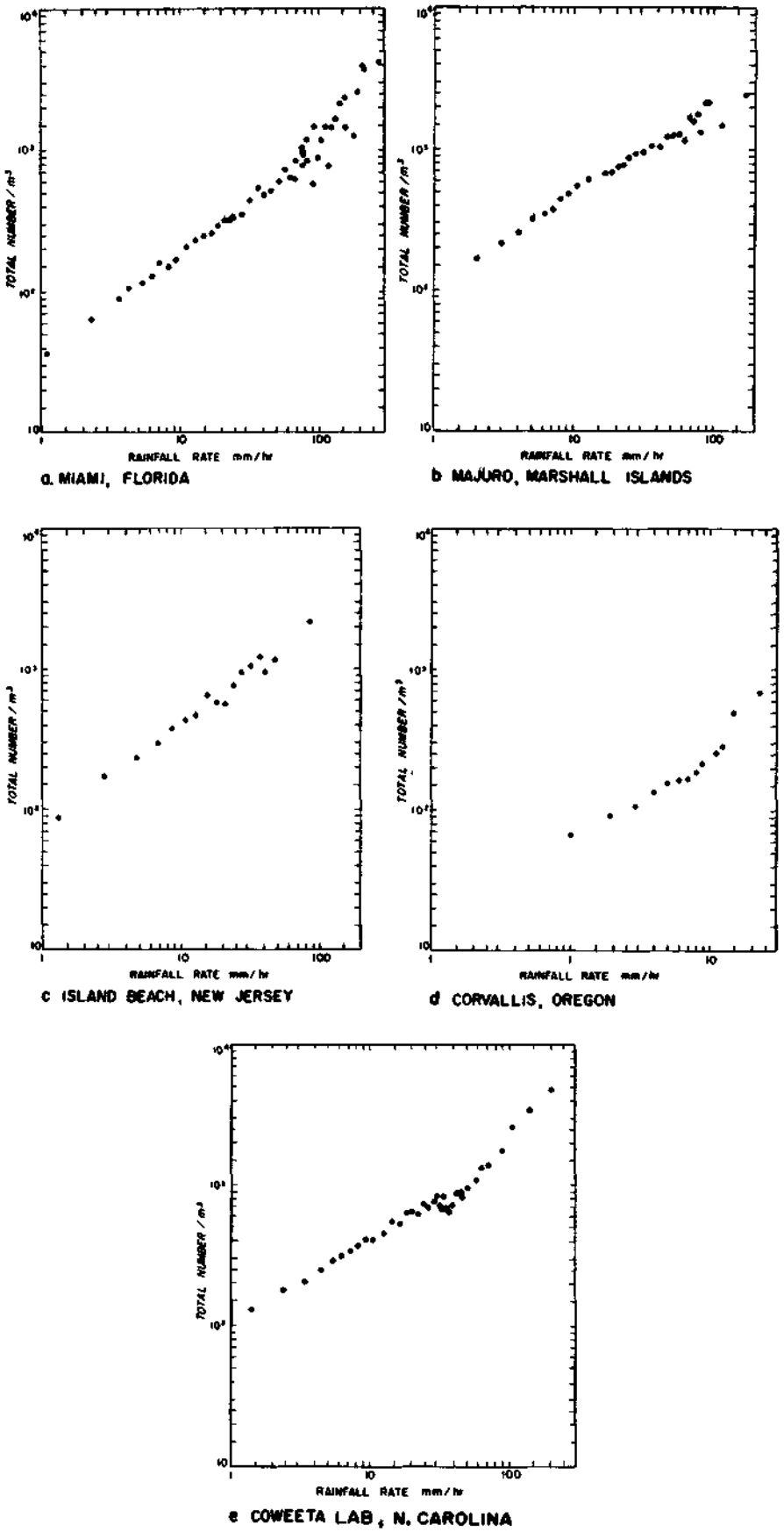

FIG. 17 NUMBER OF DROPS PER CUBIC METER VS. RAINFALL RATE

calculated rainfall rate and radar reflectivity are not greatly affected and the data has been included in the analysis.

Fitting Equations for Drop Size Distributions

Several fitting equations have been proposed for drop size distributions. Probably the best known and most widely used one is that of Marshall and Palmer.[40]

$$N_D = N_o \exp(-\Lambda D) \tag{22}$$

where N_D dD is the number of drops per cubic meter of diameter between D and D + dD mm, and N_o is the value of N_D for D = 0. N_o was considered constant with a value of 0.08 cm^{-4}. The parameter Λ was related to rainfall rate by the equation

$$\Lambda = 41\ R^{-0.21} \tag{23}$$

where R is the rainfall rate in millimeters per hour. These equations have been found very useful by many investigators due largely to their simplicity. However, the number of small drops is overestimated quite severely. Even if drops below the mode are ignored, it has been found that much of the raindrop camera data is not fitted well by these equations using a constant N_o and with Λ determined by equation (23).

Marshall and Palmer data tended to show a decrease in drops below 1.3 mm. They did not measure drops below 1.0 mm and thus the straight line appears to fit their data. If

the Marshall and Palmer relationship is fitted to the raindrop camera data for the larger drops, the slope of the lines do not vary as $R^{-.21}$. At Miami the slope remains constant or even increases slightly with large values of R. Figure 18 shows the manner in which the parameter Δ varies with rainfall rate for the Miami data. In addition, the intercept value N_o fluctuates greatly.

Fujiwara[41] proposed the equation

$$N_D = \alpha (D-D_o)^2 \exp -\beta (D-D_o)^3 \qquad (24)$$

where α, β, and D_o are empirical parameters. This equation fits the small drop portion of the distribution much better than equation (22). The major disadvantage of this form of fitting equation is the difficulty of determining the three parameters α, β, and D_o, from a distribution.

The log-normal distribution has been examined as to its applicability to drop size distributions. The use of this distribution has been suggested by Levine.[42] Also, Matvejev[43] references the work of Kolmogoroff on this equation. Irani and Callis[44] use the log-normal distribution for particle size distributions in general. This distribution has the appearance of a Gaussian normal distribution if the frequency of occurrence is plotted against the logarithm of the drop diameter.

The log normal distribution can be expressed in the following form for use with drop size distributions

$$N_D\, dD = \frac{N_T}{D\sqrt{2\pi}\ln\sigma} \exp -\frac{1}{2}\left(\frac{\ln D/D_G}{\ln \sigma}\right)^2 dD \qquad (25)$$

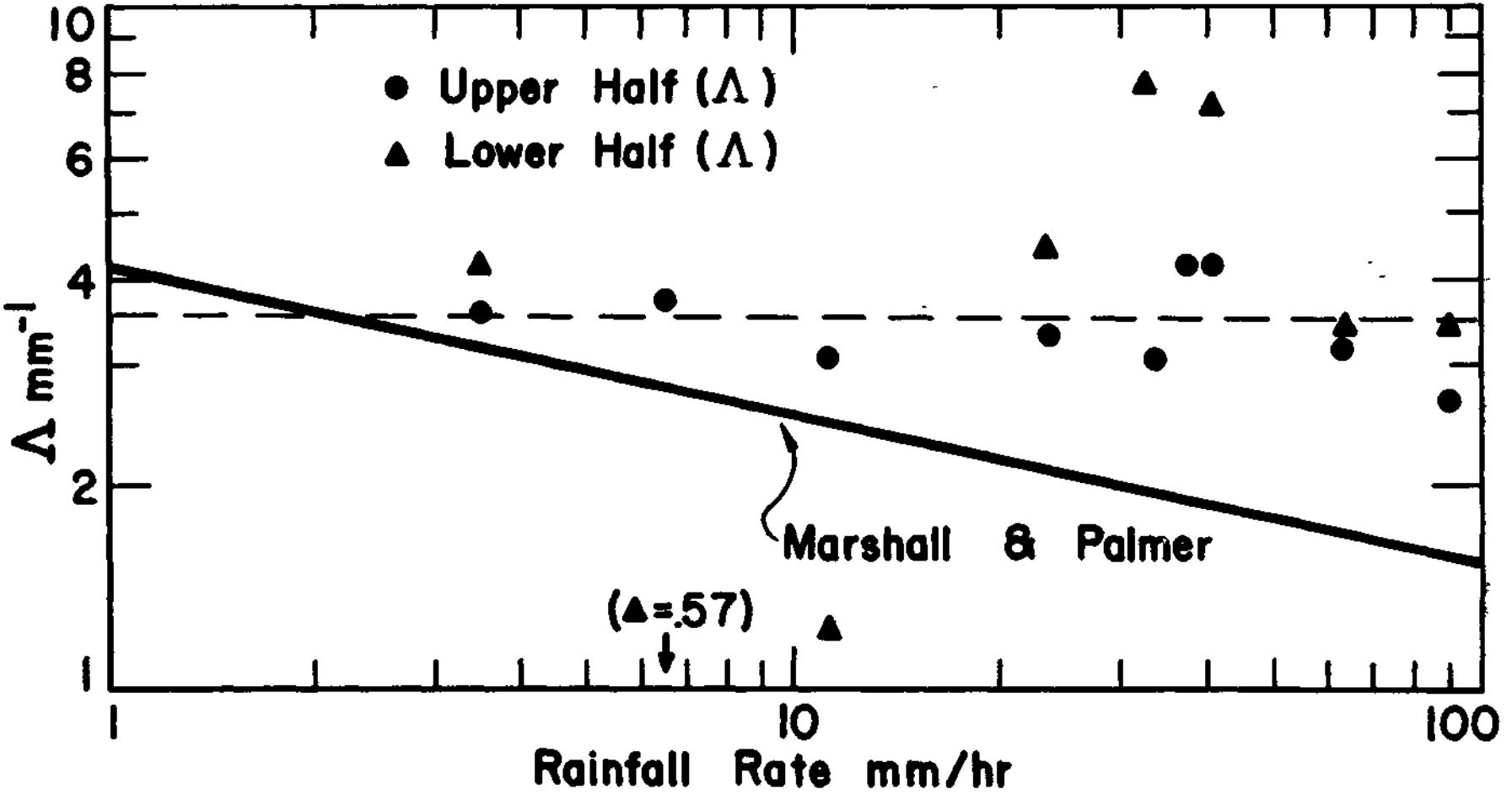

FIG. 18 VARIATION OF A WITH RAINFALL RATE

In this equation, N_D dD is the number of drops/m^3 of diameter between D and D + dD, and N_T is the total number of drops/m^3 in the distribution. D_G is the geometric mean diameter of the distribution and is readily computed from the distribution by the equation

$$\ln D_G = \frac{1}{N_T} \sum_{i=1}^{7.9} n_i \ln D_i \qquad (26)$$

The geometric standard deviation, σ, is then given by

$$\ln \sigma = \left[\frac{1}{N_T} \sum_{i=1}^{79} n_i (\ln D_i - \ln D_G)^2 \right]^{1/2} \qquad (27)$$

The average distributions were fitted by computing $\ln D_G$ and $\ln \sigma$ using equations (26) and (27); then these values were used in equation (25) to calculate the "theoretical" points on figures 9 through 16. In general, these points fit the data better than any other distribution tested. It also fits individual one-minute distributions satisfactorily. The parameters of the fitting curves can be easily determined from equations (26) and (27) and N_T by summing the number of drops in each sub class.

RESULTS OP ANALYSIS

Radar Reflectivity-Rainfall Rate Relations

The primary purpose of this research was to find a relationship between rainfall rate and radar reflectivity,, Both of these parameters were calculated from the drop size spectrum. Prior work indicated that the most appropriate relationship could be obtained by finding the regression line between the logarithms of rate and reflectivity. Most of the analysis has been performed using this technique which is called the logarithmic least squares.

This method minimizes the logarithmic (or percentage) error. The resulting equation is

$$\log R = K_0 + K_1 \log Z \tag{28}$$

where k_o and k_l are constants. Since,, for practical use of a radar set, the reflectivity is measured and used to predict the rainfall rate, the analysis was performed with reflectivity as the independent variable. With this assumption

$$K_1 = \frac{\text{cov } Z'R'}{\text{var } Z'} \tag{29}$$

where the primes indicate common logarithms of variables

and

$$K_o = \frac{1}{N}\sum_i R'_i - \frac{K_1}{N}\sum_i Z'_i \qquad (30)$$

A more common form for radar meteorological work is

$$Z = aR^b \qquad (31)$$

where $$a = 10^{k_1/k_o} \qquad (32)$$

$$b = \frac{1}{k_1} \qquad (33)$$

An estimate as to how well the data are represented by the regression lines is the correlation coefficient or the standard error of estimate. The correlation coefficient, r, is defined as

$$r = \left[\frac{cov^2 Z'R'}{var\, Z' \, var\, R'}\right]^{1/2} \qquad (34)$$

The correlation coefficient for this data is always high, varying from 0.90 to 0.99. The standard error of estimate, S_e, is obtained by

$$S_e = \left[(var\, R')(1 - r^2)\right]^{1/2} \qquad (35)$$

This latter statistic may be interpreted as a measure of the amount of scatter around the regression line. If this scatter is Gaussian, then S_e is the best unbiased estimator of the standard error of the deviations of the data points from the regression line,, This measure is not completely justifiable since the variation of the points around the regression is not normally distributed. Nevertheless, its use appears reasonable in estimating the relative reliability of the different data stratifications which are made in the following sections. Figures 19 through 24 are plots of the data points and the fitted curves. Not every data point is plotted since there are so many points. On the right of each figure is an indication of the plotting density used. The points plotted were chosen at random. The scatter of points around the regression line is larger for the low rates and reflectivity. This greater scatter is probably due to larger sample error in the low rates and to the logarithmic transformation which tends to exaggerate the differences of a rate when the rate is low.

A second technique was also used which removed the somewhat arbitrary form of the result. This method consisted of ranking a group of data by reflectivity. The ranked data was then separated into intervals of the reflectivity. These intervals were chosen to be 1 db wide. This choice is dictated by the means used in calibrating radar sets which normally yield calibrations in the logarithmic units. Separation at arithmetic intervals was performed and the results are similar.

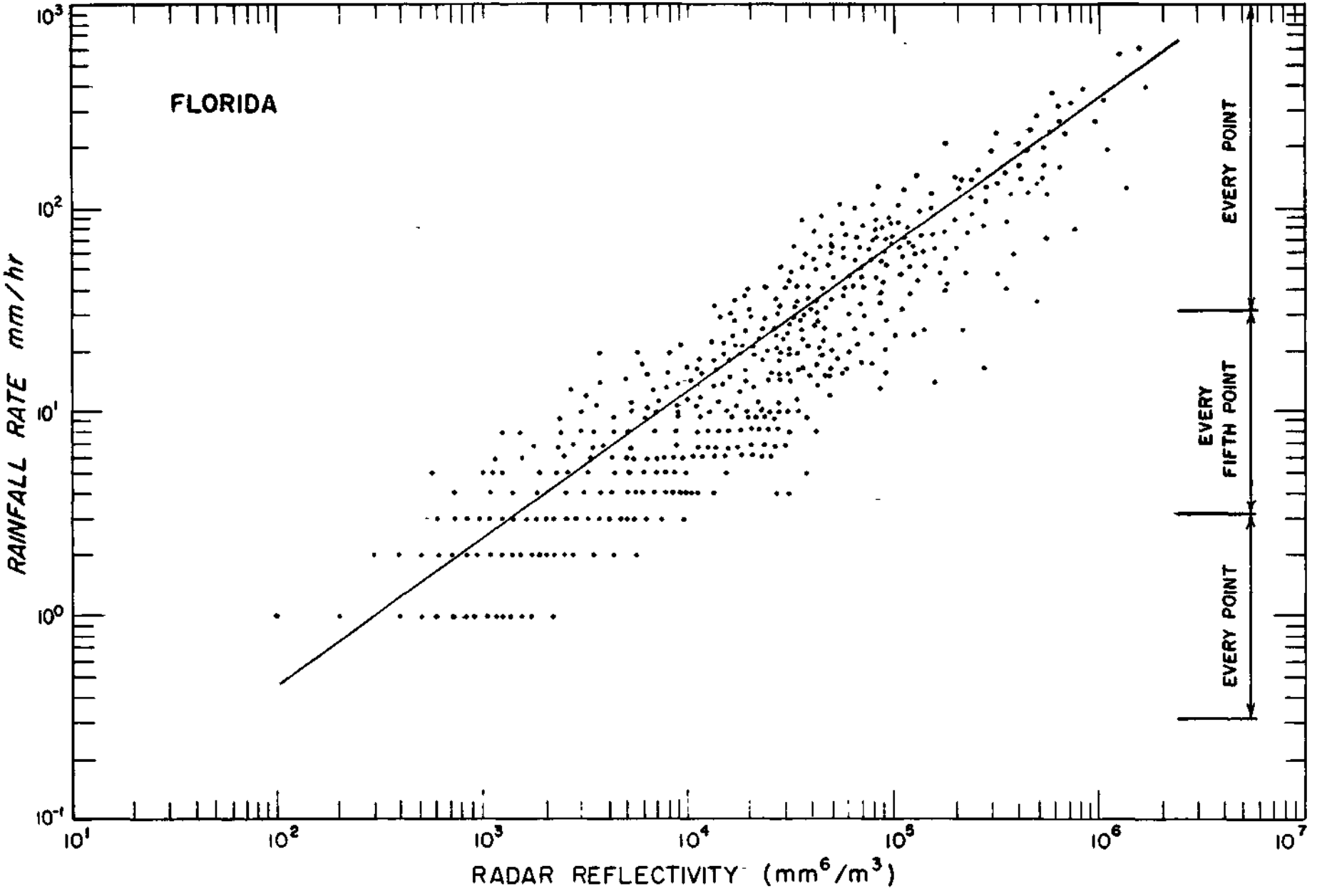

FIG. 19 RAINFALL RATE- RADAR REFLECTIVITY SCATTERGRAM FOR FLORIDA DATA

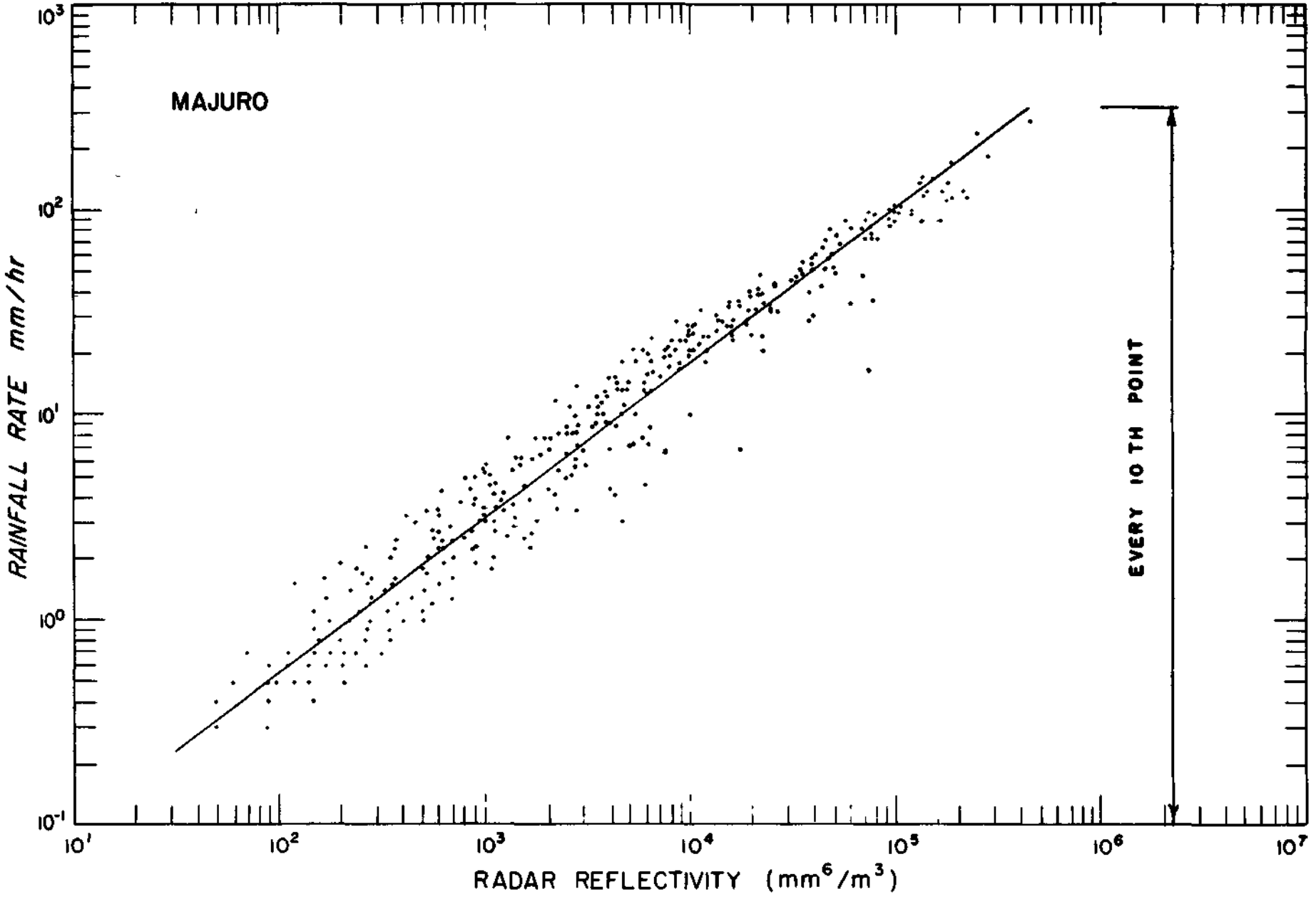

FIG. 20 RAINFALL RATE - RADAR REFLECTIVITY SCATTERGRAM FOR MAJURO DATA

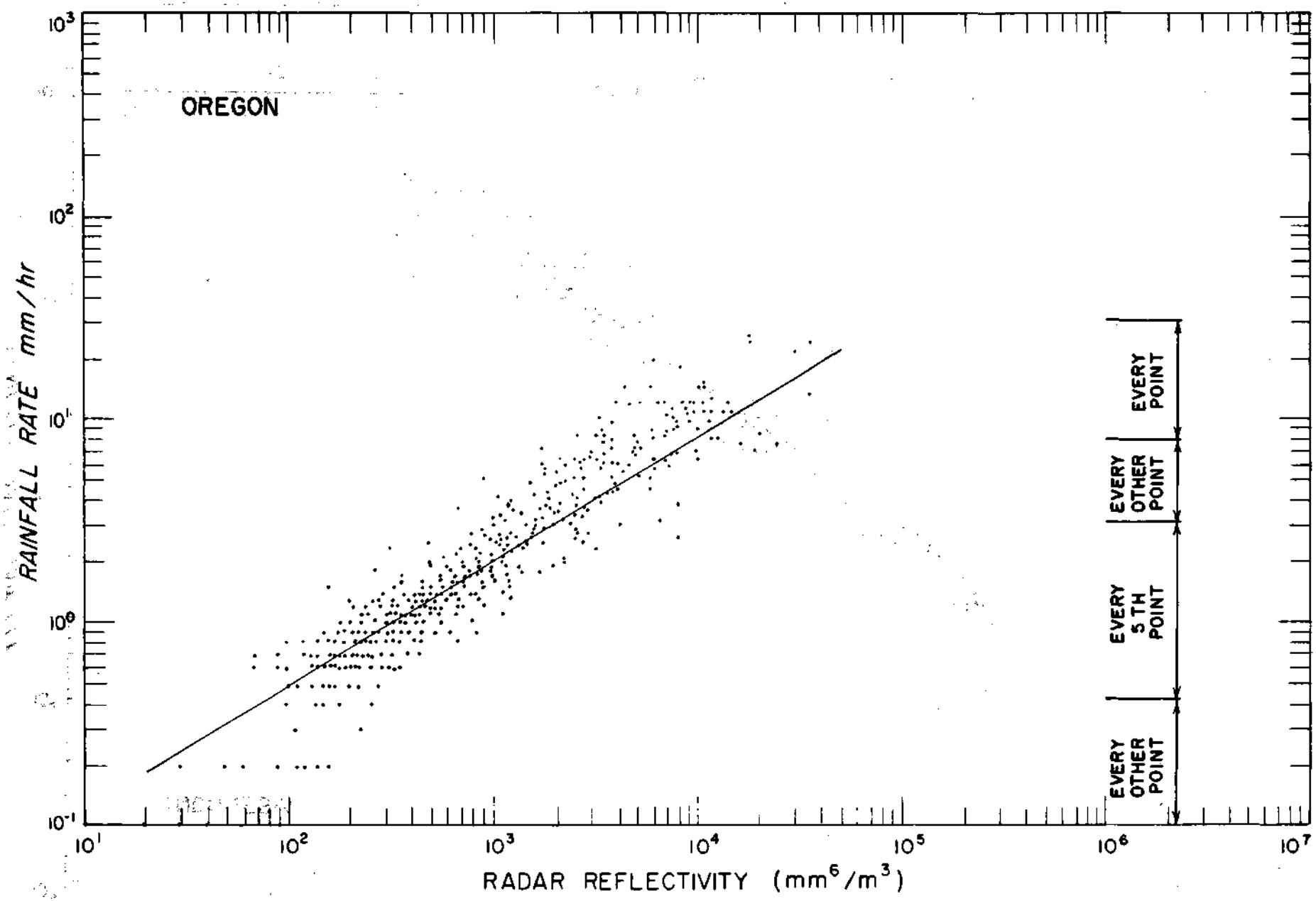

FIG. 21 RAINFALL RATE- RADAR REFLECTIVITY SCATTERGRAM FOR OREGON DATA

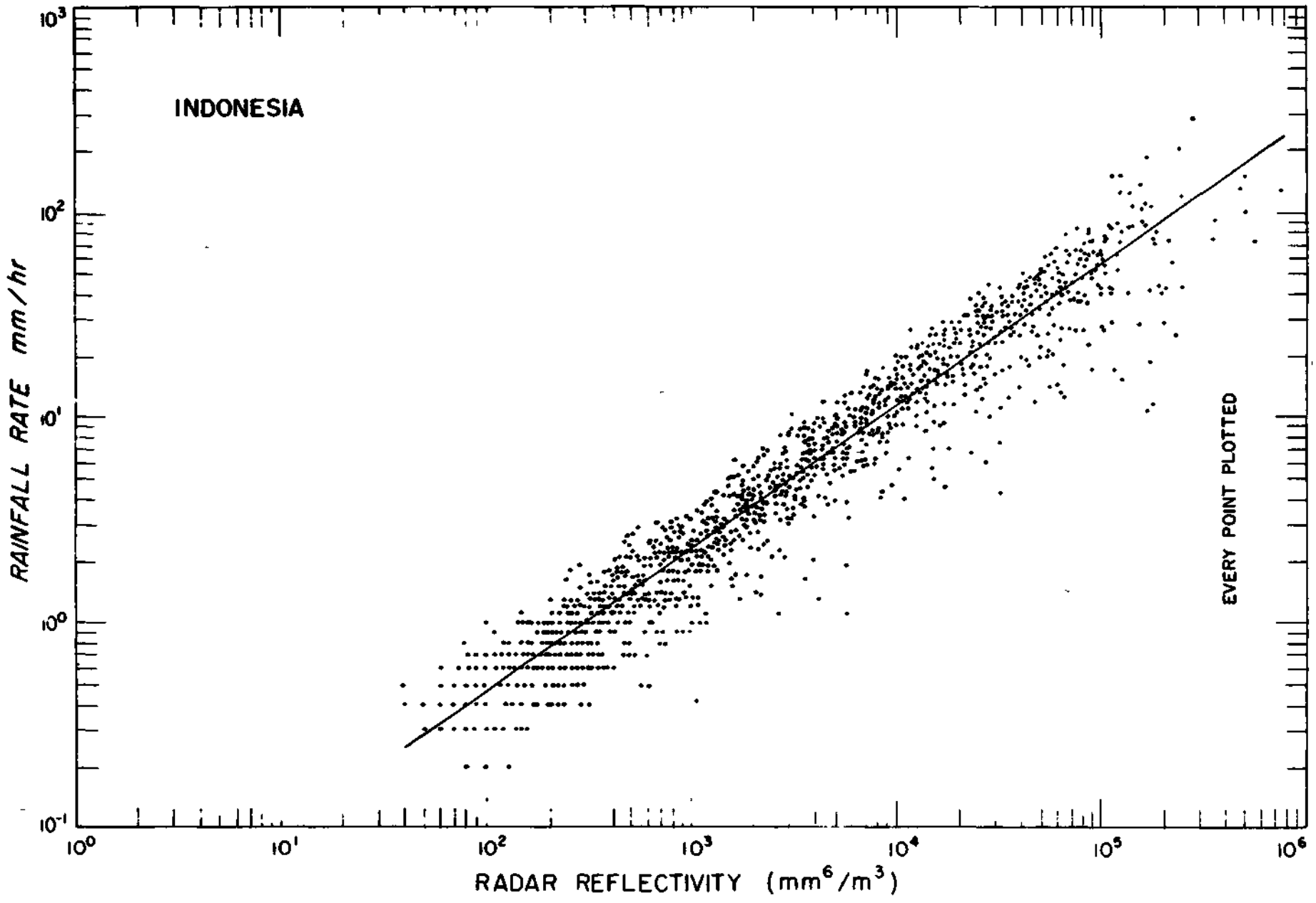

FIG. 22 RAINFALL RATE - RADAR REFLECTIVITY SCATTERGRAM FOR INDONESIA DATA

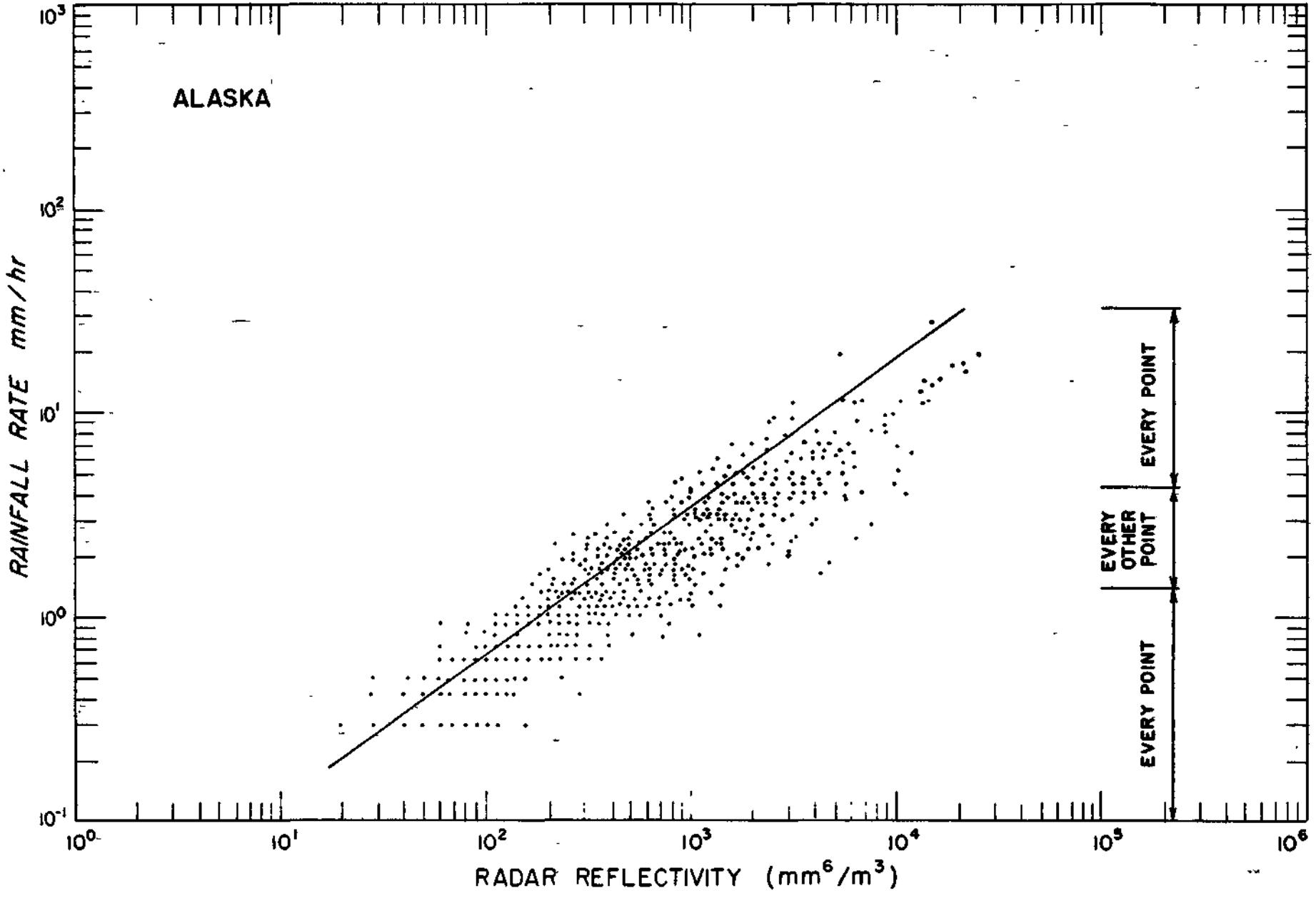

FIG. 23 RAINFALL RATE - RADAR REFLECTIVITY SCATTERGRAM FOR ALASKA DATA

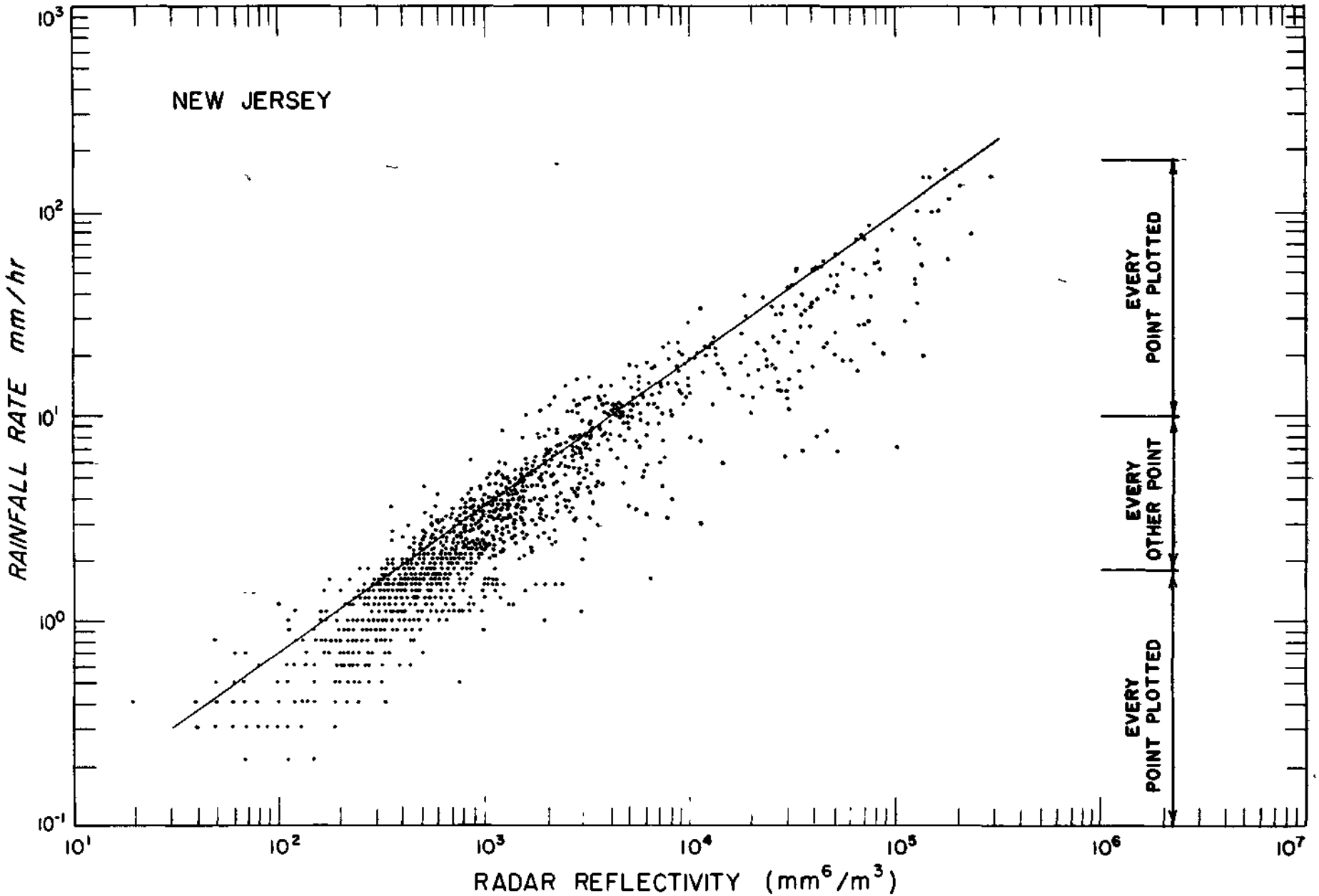

FIG. 24 RAINFALL RATE-RADAR REFLECTIVITY SCATTERGRAM FOR NEW JERSEY DATA

Within each interval, the average rainfall rate was determined. This average rate is then considered to be the best estimate of rate for this value of reflectivity.

Non-Stratified Relations

The relationships for the entire data sample for each location are shown in table 2. Even though the correlation coefficients are as high as 0.98, the data is scattered over rainfall rate range of a factor of three. This accuracy is not sufficient for many purposes although it may be sufficient for some. A standard error of estimate of 0.198, as at Florida, indicates that logarithmic values greater by 0.198 occur with a priori probability of 0.68. An increase of the logarithm by 0.198 is an increase in the number by 1.57 times.

TABLE 2

RADAR REFLECTIVITY-RAINFALL RATE RELATIONS FOR NON-STRATIFIED DATA

Location	$Z = aR^b$ a	b	Correlation Coefficient	Standard Error of Estimate
Florida	286	1.43	0.95	0.198
Marshall Islands	221	1.32	0.96	0.170
Oregon	301	1.64	0.92	0.136
Indonesia	311	1.44	0.98	0.147
Alaska	267	1.54	0.94	0.142
North Carolina	230	1.40	0.97	0.171

The second method of analysis is presented in abbreviated form in table 3 for six locations. A Z interval of 1 db was used but the results of every fifth interval only are presented for brevity. These values when plotted on log-log graph paper produce straight lines not different from the regression

lines found from logarithmic least squares. Since these yield straight lines the logarithmic least squares is an acceptable analysis method and does not appear to be improperly forcing the data to a straight line.

TABLE 3

MEAN RAINFALL RATES AS A FUNCTION OF REFLECTIVITY

Reflectivity (mm^6/m^3)	Florida	Marshall Islands	Oregon	(mm/hr) Indonesia	Alaska	North Carolina
$1.1 \cdot 10$	1.0	1.0	0.6	0.5	0.6	0.6
$3.5 \cdot 10$	1.0	1.6	1.1	l.l	1.2	1.6
$l.l \cdot lO^2$	2.5	3.7	2.3	2.4	2.8	3.5
$3.5 \cdot 10^2$	6.3	8.7	5.4	6.0	5.2	7.8
$l.l \cdot 10^3$	14.5	21.6	9.5	14.4	8.8	17.7
$3.5 \cdot 10^3$	34.8	48.4	18.7	29.5	9.0	38.7
$1.1 \cdot 10^4$	68.5	90.5	-	65.7	9.2	87.1
$3.5 \cdot 10^4$	167.1	-	-	70.0	-	-
$1.1 \cdot 10^5$	247.7	-	-	123.8	-	-

A number of differences between locations can be seen in these non-stratified data. The two extreme locations are the Marshall Islands and Alaska. The Marshall Island data indicate the highest rainfall rate for a particular radar reflectivity. At a reflectivity of $1.1.10^4$ mm^6/m^3, nearly 10 times greater rainfall rate is occurring In the Marshall Island climate than in the climate around Alaska. The drop size spectra In the Marshall Islands contain a relatively large number of small droplets which do not yield as much radar return as the larger but fewer drops in the Alaskan rains.

The climate of Oregon is similar to that of Alaska and thus the relationships are very similar. Florida and Indonesia

tend to be nearly the same for low and medium values of the reflectivity but for the high values Florida has higher rates. This departure at the high rates is suggestive that different meteorological conditions prevail during high rate conditions at these locations.

Stratification by Rain Type

At some locations the data were separated into groups according to the rain type classification as reported by the observer operating the camera. The rain types recognized were thunderstorms, rainshowers, and continuous rain. The observers in all cases had had some form of weather training and their reports were not modified.

The camera at North Carolina was operated on the side of a mountain some 4 miles from the observer's normal duty station. This prevented him from making observations of the rain type occurring at the camera. The observers at Alaska reported continuous rain for nearly all of the data and there was not sufficient data in the rainshowers to allow meaningful regressions. At the other extreme, nearly all of the data from Indonesia was reported as thunderstorms. At the remaining locations, stratification by rain type was performed and the results of the logarithmic least squares are shown in table 4.

Since the standard error does not decrease appreciably, this stratification does not benefit the user greatly. The more showery a rain becomes the higher the radar reflectivity

for medium to high rates. This is indicated by the increase in the size of the exponent from continuous rain through showers to the thunderstorms.

TABLE 4

RADAR REFLECTIVITY-RAINFALL RATE RELATIONS
USING RAIN TYPE STRATIFICATIONS

Location	Rain Type	$Z = aR^b$ a	b	Correlation Coefficient	Standard Error of Estimate	Minutes of Data
Florida	Continuous	322	1.33	0.94	0.187	911
	Showers	250	1.47	0.95	0.185	696
	Thunderstorms	224	1.51	0.94	0.190	902
Marshall Islands	Continuous	226	1.46	0.97	0.184	1491
	Showers	146	1.42	0.92	0.141	952
Oregon	Continuous	295	1.59	0.92	0.133	600
	Showers	327	1.66	0.91	0.135	218
	Thunderstorms	339	1.64	0.95	0.089	82

Stratification by Synoptic Type

Stratification of data by examining the surface meteorological chart prepared by the U. S. Weather Bureau was attempted. The classification was in accordance to the major disturbance in the area and its relative position to the camera. A partial list of the classifications is air mass, pre-cold frontal, cold frontal, post-cold frontal, warm front, overrunning, Easterly Wave, trough aloft, warm occlusion, cold occlusion, trade wind showers, and intertropical convergent zone. Naturally, not all of these classes were filled at any one location. Surface maps were not available for Indonesia so this could not be performed. Data from Alaska and North Carolina have not been stratified by synoptic type due to lack of analysis time.

Table 5 presents the results of the synoptic stratifications for the other locations.

TABLE 5

RADAR REFLECTIVITY-RAINFALL RATE RELATIONS USING SYNOPTIC STRATIFICATIONS

Location	Synoptic Class	$Z = aR^b$ a	b	Correlation Coefficient	Standard Error of Estimate	Minutes of Data
Florida	Air Mass	323	1.42	0.98	0.180	467
	Pre-Cold Front	280	1.49	0.95	0.188	744
	Cold Front	198	1.54	0.95	0.176	187
	Warm Front	403	1.24	0.96	0.145	341
	Overrunning	302	1.36	0.94	0.165	196
	Easterly Wave	296	1.35	0.97	0.156	536
	Trough Aloft	261	1.43	0.97	O.178	80
	Pre-Cold Occlusion	330	1.66	0.91	0.127	40
Marshall Islands	Easterly Wave	196	1.38	0.95	0.171	1126 /
	Trade Wind Showers	126	1.47	0.98	0.130	239
	Intertropical Convergence Zone	196	1.38	0.95	O.178	1136
Oregon	Air Mass	322	1.62	0.95	0.094	157
	Post-Cold Front	322	1.70	0.90	0.140	204
	Overrunning	307	1.56	0.92	0.138	352
	Warm Front	295	1.66	0.91	0.143	158
	Warm Occlusion	339	1.48	0.95	0.126	175
	Pre-Warm Occlusion	309	1.92	0.90	0.111	151
	Post-Warm Occlusion	268	1.81	0.88	0.146	320

Some improvement is suggested in this stratification scheme. The standard errors do reduce somewhat and the correlation coefficients generally are slightly higher. Some reduction in the standard error of estimate might be expected as a result of smaller sample. Confidence limits calculated for the exponent, b, would indicate that the chances are remote that these are samples of the same parent population.

Stratification by Thermodynamic Instability

The conditions of the air aloft influence the production of raindrops. A measure of the instability of the air was investigated to determine whether a significant reduction of the standard error of estimate could be obtained. The thermodynamic instability to some extent measures the strength of updrafts and available moisture. Tornado forecasts are based partially on this instability. The vigor of the storm might be reflected in the drop size spectra. A measure of the thermodynamic instability is the amount of energy required to lift a parcel of air from the ground to a prescribed level aloft. If this energy is negative, instability is indicated. In the calculations parcels of air were raised from the surface and from every 50 mb pressure level to 600 mb up to a pressure height of 150 mb. The sum of the energies for each of the parcels is then a measure of the average thermodynamic instability. Radiosonde observations are normally obtained every 12 hours. The nearest earlier radiosonde was used for each storm. The range of instabilities was then divided into groups and logarithmic least square analysis performed on each group. Table 6 contains the result of this analysis. The standard error of estimate is generally larger for this stratification than for either the synoptic type or the rain type stratification. One of the errors which may contribute to this poor stratification is the time separation between the radiosonde ascent and the time of rainfall. Frequently, the upper air conditions change just before the rain occurs.

Indeed, the change in the upper air conditions may produce the rainfall.

TABLE 6

RADAR REFLECTIVITY-RAINFALL RATE RELATIONS USING THERMODYNAMIC INSTABILITY STRATIFICATION

Location	Instability	$Z - aR^b$ a	b	Correlation Coefficient	Standard Error of Estimate	Minutes of Data
Florida	1 (highest)	264	1.40	0.97	0.141	136
	2	295	1.36	0.97	0.169	286
	3	307	1.41	0.97	0.150	367
	4	304	1.41	0.96	0.168	416
	5	313	1.39	0.98	0.141	133
	6	206	1.42	0.97	0.105	117
	7	420	1.41	0.97	0.191	161
	8	358	1.31	0.95	0.155	559
	9	352	1.38	0.95	0.146	238
	10 (lowest)	257	1.27	0.96	0.175	167
Marshall Islands	1 (highest)	153	1.38	0.97	0.182	160
	2	207	1.47	0.92	0.241	303
	3	143	1.41	0.97	0.182	356
	4	234	1.36	0.92	0.250	736
	5	172	1.41	0.94	0.227	738
	6	191	1.40	0.96	0.226	76
	7 (lowest)	166	1.46	0.96	0.218	91
Oregon	1 (highest)	237	1.98	0.86	0.143	32
	2	216	2.01	0.88	0.127	36
	3	217	1.51	0.92	0.136	79
	4	211	1.99	0.86	0.146	369
	5	167	3.05	0.76	0.109	101
	6	232	1.98	0.83	0.160	182
	7	263	1.66	0.88	0.163	99
	8 ([lowest)	248	1.90	0.88	0.147	526

The inadequacies of the radiosonde data along with the loss of accuracy as estimated by the standard error of estimate preclude the use of this stratification.

LIQUID WATER CONTENT

As a secondary study the liquid water content for various rainfall rates were computed. This part of the study was accomplished at the request of the Naval Turbine Test Center as an aid in the operation of jet aircraft in rain. High values of liquid water content ingested by an aircraft turbine engine produce "flame out" and "compressor stalls." The raindrop size spectra were used to calculate the mass of water per cubic meter of air space. The liquid water content was then compared with the rainfall rate. Figure 25 shows liquid water content plotted against rainfall rate for Illinois, Florida, and Alaska. Each point on these graphs shows the average liquid water content for each 1 mm/hr increment of rainfall rate up to 100 mm/hr. Above this rate, larger increments are used. The logarithmic least squares fit to the Florida data produces the equation

$$L = .0528\ R^{0.95} \tag{36}$$

where

L is the liquid water content in gm/m^3

R is the rainfall rate in mm/hr.

Plotted on the graph for Florida are the highest and lowest value of liquid water content associated with each rainfall rate up to 100 mm/hr. Above this rate, the scatter about the points becomes so small on logarithmic paper that it has not been plotted. The value of the exponent of the rate being near unity is an indication that a linear relationship

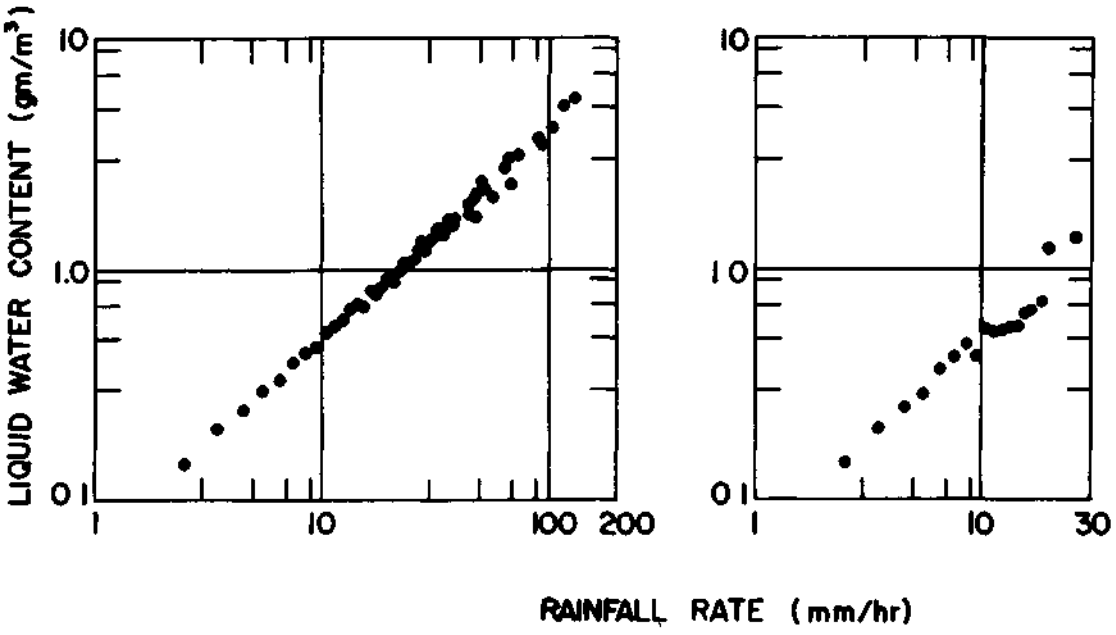

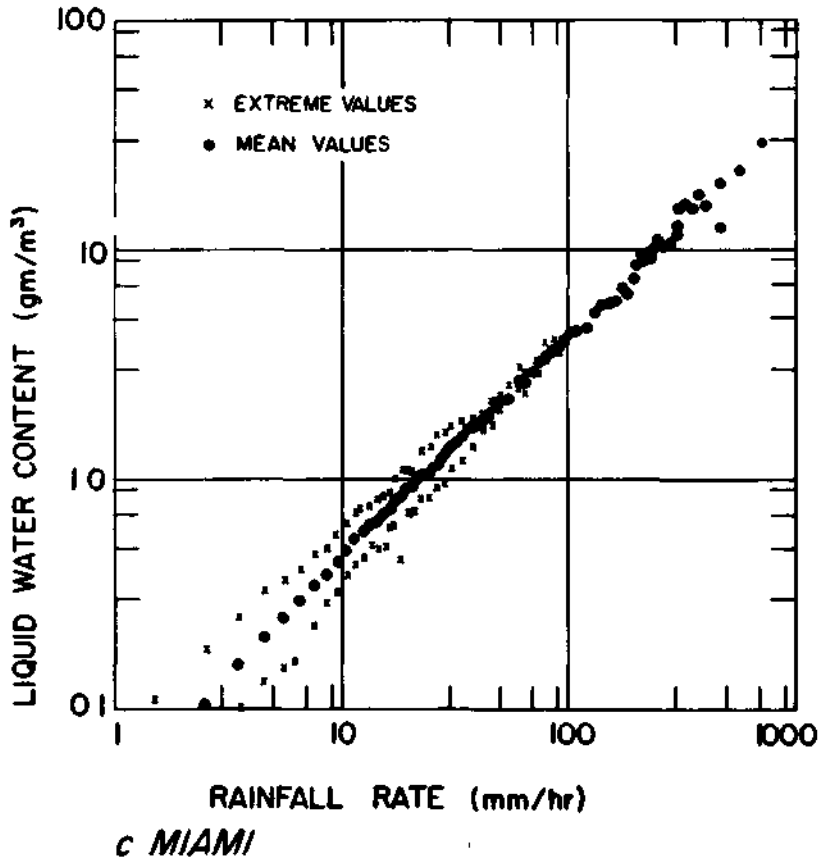

FIG 25 LIQUID WATER CONTENT VERSUS RAINFALL RATE FROM FLORIDA, ILLINOIS & ALASKA.

between these parameters would be as adequate as the logarithmic equation,, A linear fit of the data yields an equation of

$$L = 0.0425\ R \qquad (37)$$

The normal jet engine can ingest liquid water up to about 10 g/m^3 before malfunctioning. This would indicate that rains with rates in excess of 200 mm/hr could be dangerous.

A second statistic of the relative frequency of occurrence of the liquid water content was desired. In general, a one-year sampling of the data was obtained at each location. During this one-year interval between 60 and 80 percent of total rainfall time was sampled. The value of a one-year sample to obtain a frequency of occurrence is doubtful since one heavy rain may seriously effect the results. Nonetheless, the frequencies were calculated as the best estimates presently available. A better method might have been to use long time frequency of rainfall records and transform them to rainfall rates by means of equation (36). This scheme could not be performed because the required rainfall rate statistics are not available in the literature.

The resulting frequency distributions are exhibited in figures 26 and 27. On inspection, it can be noted that there are groups of data that appear to be very similar. The frequency distributions from Alaska and Oregon are nearly duplicates of each other. They both represent very light rainfall and low liquid water content. Marshall Islands and Indonesia, both representative of tropical conditions, also appear to be

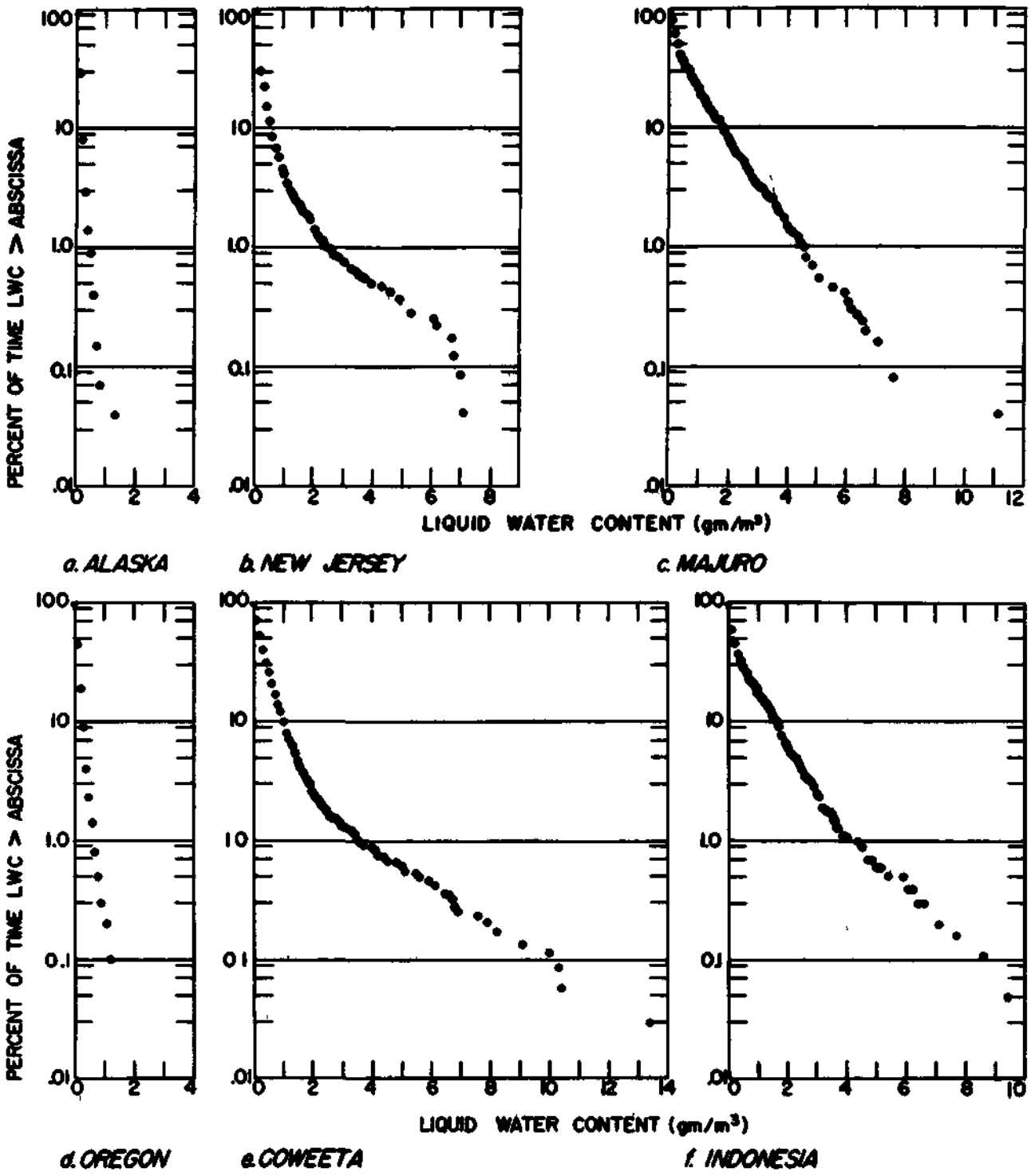

FIG 26 LIQUID WATER CONTENT FREQUENCY DISTRIBUTIONS

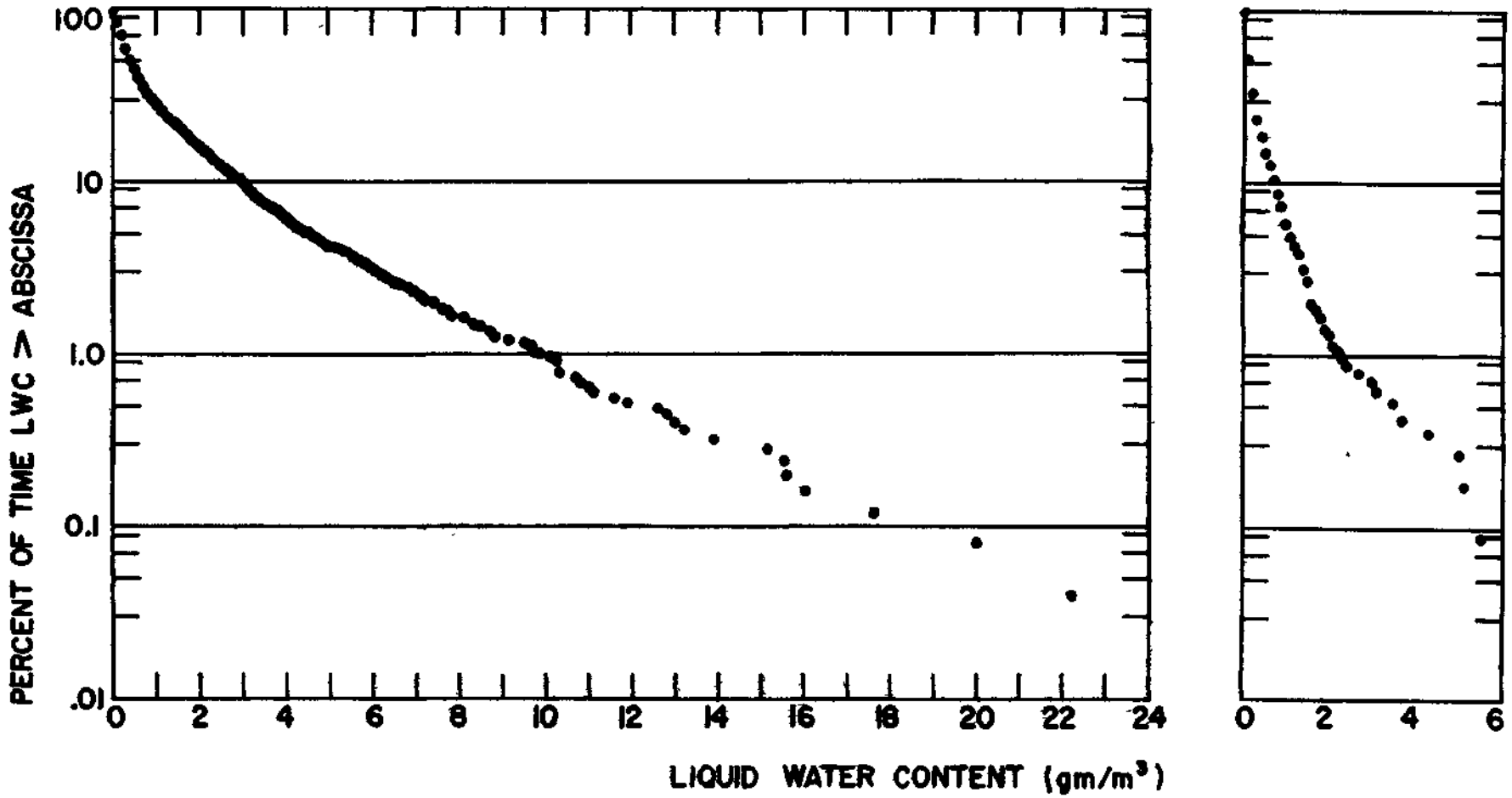

a. MIAMI

b. ILLINOIS

FIG. 27 LIQUID WATER CONTENT FREQUENCY DISTRIBUTIONS

very similar. They both appear to be nearly straight on these plots and there is less than .05 g/m^3 spread between them at any point except at the highest liquid water content points. These points are subject to large sampling error since only a few samples were obtained at these values. Likewise, New Jersey and North Carolina seem to be very similar, again, differing primarily in the higher values of liquid water content. Both New Jersey and North Carolina exhibit a curvature in the low liquid water content region. The data from Marshall Islands are all shower type rainfall. The Indonesia data are thunderstorms and showers. Therefore, it would appear that showers and thunderstorms can be characterized by a straight line with low slope on these distributions. If it is noted that the curves for Alaska and Oregon represent, primarily, continuous rains and that they represent very high values of the ordinate for low liquid water content, 1½ grams per cubic meter and below, an explanation for the curvature in the New Jersey and North Carolina data might be obtained. It is proposed that a portion of the New Jersey and North Carolina rain were of a light continuous nature, similar to the light continuous rains found at Alaska and Oregon. Thus, when these are added to the showery rainfalls as represented by the data from Majuro and Indonesia, a curve such as those for New Jersey and North Carolina is obtained.

The curve from Miami, Florida, is different from any of those previously described. It does have some curvature at

the small end which might be attributed to light continuous rain, but it has a much higher percentage of the rains occurring with large liquid water content than either Majuro or Indonesia.

The highest liquid water content was obtained at Miami and was 29.18 g/m^3. This point does not show on the figure since the probability of higher amounts is extremely low.* The portion of the curve beyond 15 g/m^3 was represented by a number of samples and it is not believed that this could have been a sampling problem in the raindrop cameras. These values are higher than any of the liquid water contents from other locations. About one percent of the rain time at Miami has liquid water contents considered dangerous to jet aircraft operation. It is believed that Miami has a unique position in that a plentiful moisture supply is available along with high instability, due to cooler, drier air aloft.

*This sample also had the highest rainfall rate measured at any locations 722 mm/hr„ The observation was made at 1426 EST, 13 May 1958. The cubic meter sample contained 4782 drops.

RADAR ATTENUATION

Raindrops produce attenuation to electromagnetic radiation as well as reflected power. This attenuation is important for wavelengths less than 5.0 cm. Since there are many weather radars operating with shorter wavelengths, a study of the attenuation by rainfall was accomplished. This work has been performed at a wavelength of 3.2 cm only. This frequency is the frequency commonly used at which attenuation is important.

Attenuation Cross Section-Reflectivity Relations

The attenuation cross section was compared with the radar reflectivity and the rainfall rate. The relationship between the radar reflectivity and the attenuation permits correction for the attenuation to be made from the power return to the radar from intervening precipitation. The technique of attenuation correction is dangerous, as small errors may become greatly magnified, eliminating all advantages of the correction. The problem of attenuation correction is discussed at length by Hitschfeld and Bordan.[45] This analysis is based on fully compensating the attenuation at each point by the calculated rainfall rates at all radial points closer to the radar. Since some of these points have already been corrected for the rain attenuation, the error is a product of the errors made previously. This cumulative error can increase without bounds. One proposal which prevents enormous errors is to correct the attenuation by the reflectivity values obtained nearer the radar but without correcting the prior values for

attenuation. This scheme will produce an undercorrection for the attenuation but will not allow the increase without bounds which occur so easily using the fully corrected technique.

The attenuation, A, in decibels per kilometer is obtained from the radar attenuation cross section by the relationship

$$A = 4.35 \cdot 10^{-3} Q \tag{38}$$

where Q is measured in square millimeters per cubic meter and A is in decibels per kilometer. The logarithmic regression of attenuation cross section on A for the various locations are presented in table 7.

TABLE 7

ATTENUATION CROSS SECTION-REFLECTIVITY RELATIONS FOR NON-STRATIFIED DATA

Location	$Q = cZ^d$ c	d	Correlation Coefficient	Standard Error of Estimate
Florida	$1.15 \cdot 10^{-2}$	0.91	0.98	0.135
Marshall Islands	$1.48 \cdot 10^{-2}$	0.90	0.99	0.089
Oregon	$2.59 \cdot 10^{-2}$	0.80	0.92	0.188
Indonesia	$1.51 \cdot 10^{-2}$	0.88	0.99	0.108
Alaska	$3.12 \cdot 10^{-2}$	0.763	0.96	0.109
North Carolina	$1.87 \cdot 10^{-2}$	0.86	0.99	0.101

Radar Attenuation-Rainfall Rate Relations

In order to compare radar attenuation values with previous work, the attenuation was compared with the rainfall rate. The commonly accepted work on attenuation is that of Robertson and King.[46] The data was separated into one millimeter per hour intervals of the rainfall rate and the average Q for each interval calculated. These points are plotted for

the Florida data in figure 28. Also plotted are the limits within which all of the Robertson and King values occur. The Robertson and King data were obtained by direct measurement of the attenuation over a path. The rainfall rate values were measured by raingages. The major discrepancies between this data and the Robertson and King data is at the rainfall rates below 8 mm/hr. At these rates the attenuation is not severe and practically of little value. A rainstorm with a depth of 20 miles and a rate of 3 mm/hr would produce an attenuation of 0.6 db. This is below the usual measurement accuracy of the radar. At higher rates the comparison of results is good. The extreme values of the drop size data produce scatter around the points of about the same order of magnitude as Robertson and King limits. A logarithmic regression yielded the equation

$$A = 1.06 \cdot 10^{-2} R^{1.22} \qquad (39)$$

with a correlation coefficient of 0.97. This line is plotted on figure 28. The attenuation at 3.2 cm wavelength can become appreciable. Rainstorms with a rate of 50 mm/hr and a depth of 10 miles produce an attenuation of 12.6 db. Use of this wavelength for measuring heavy precipitation rates is not advisable. However, consideration of radar size and performance often dictate these shorter wavelengths. If these short wavelengths are used, proper precautions and partial correction for rain attenuation appear advisable.

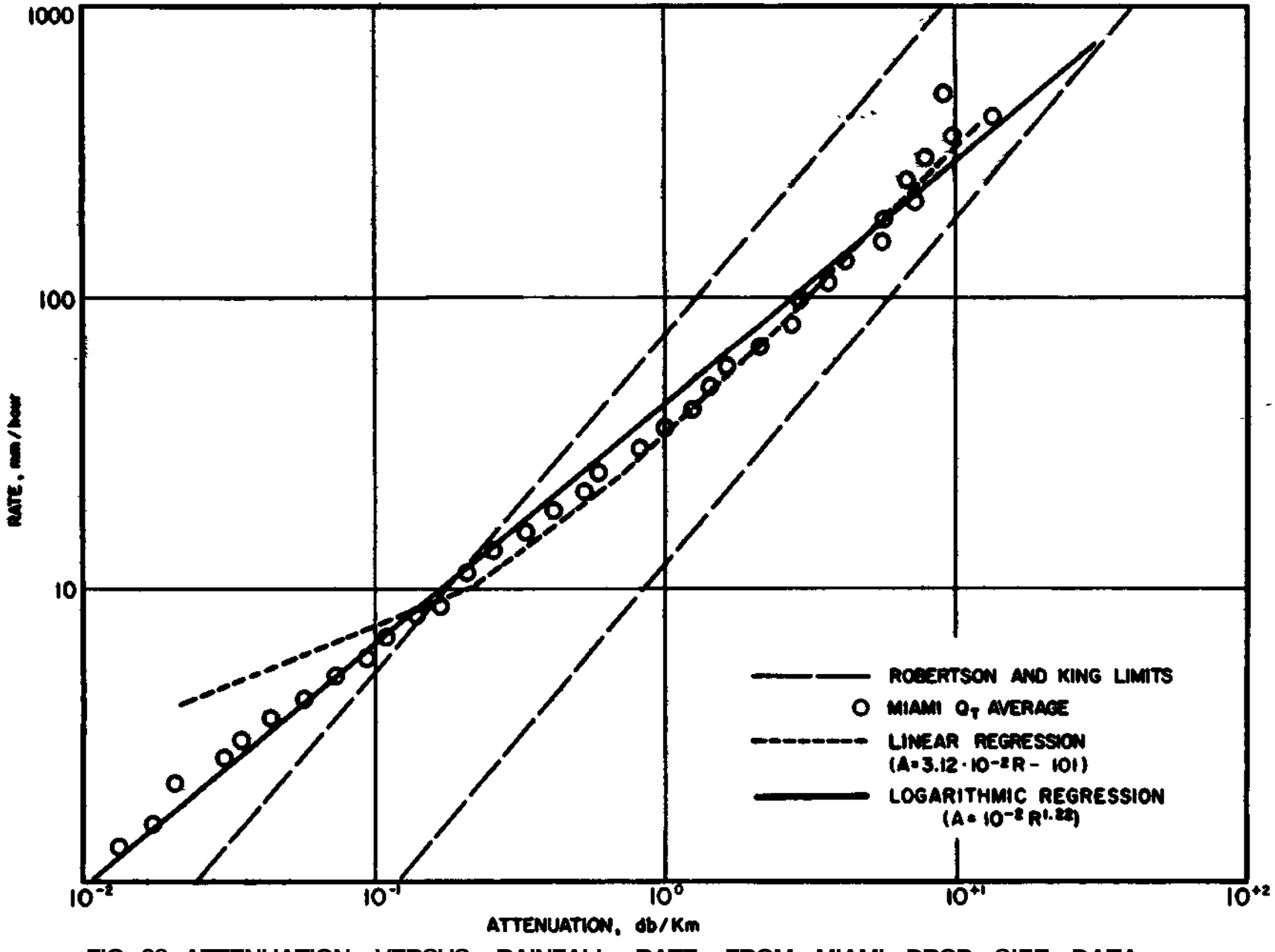

FIG. 28 ATTENUATION VERSUS RAINFALL RATE FROM MIAMI DROP SIZE DATA.

CONCLUSIONS AND RECOMMENDATIONS

A number of factors other than the drop size spectra have a decided effect on the accuracy with which a radar can measure rainfall rate. A partial list of these other factors is:

(a) Calibration accuracy of transmitter power, receiver sensitivity, and antenna gain

(b) Processing inaccuracies in obtaining the true average power return from a point in space

(c) Uncertainty that the radar volume is filled with precipitation echo at the same rainfall rate

(d) Precipitation attenuation if shorter wavelengths are used

(e) Abnormal transmission paths between the radar and rainfall of interest.

All statements in this paper with regards to accuracy of a radar's estimate of rainfall rate will not consider uncertainties due to any of these problems. The remaining variation is one of varying drop size distributions for the same rainfall rate. If the radar volume was a volume of 1 m^3, the standard error of estimate would provide a good measure of the possible accuracies of estimating the rainfall rate from the radar return. For non-stratified data the standard error of estimate of the logarithms was between 0.136 and 0.198. Thus, the logarithm of R could be estimated to within ±0.198

sixty-eight percent of the time. This result can be restated as; the rate obtained would be from 63 percent low to 57 percent high, sixty-eight percent of the time. Fortunately, a radar set samples a much larger volume. If a large amount of the scatter around the regression lines is due to the relatively small volume sampled by the raindrop camera, this larger volume will produce a much smaller error. Data have been obtained to test this hypothesis but the analysis has not been completed. Preliminary results indicate that the standard error of estimate will be reduced by at least a factor of two if a sampling volume of 8 m^3 is obtained from the same storm in one minute's time. Since the radar samples a volume of the order of 10^5 m^3, the standard error should be reduced by at least 10 times if the variance is all due to sample size. If this is so, the accuracies should be within ±5 percent. More likely there is variance in the non-stratified data due to effects other than sample size. These variances can be removed only by stratifying the data. Choosing the appropriate criteria for stratifying is complicated by the large scatter due to sample size. The only practical method appears to be trial and error.

The results from different climatic areas indicate that a different relationship must be used for different localities if large errors are to be avoided. The differences between Alaska and the Marshall Islands illustrate this vividly. Differences between these localities was anticipated, but not of this large a magnitude. Radar operators of the U. S.

Army had indicated that large amounts of return signal were experienced in Alaska even though only low to moderate rainfall rates were occurring.

A slight improvement in accuracy can be obtained by using different relationships chosen with regards to meteorological parameters. At some locations, Alaska and Oregon for instance, the improvement is not great. In comparison the standard error of estimate at Florida can be reduced from O.198 to about 0.16 by stratifying by synoptic types. This reduction may be even more important than is suggested by this reduction since the variance removed is variance from a source other than from small sample size. Thus, after stratification the large sample of a radar volume may actually have considerably smaller residuals than if stratification had not been performed. The stratification by thermodynamic instability did not improve the estimates as much as synoptic sorting. Often the rain type sorting is the most easily applied for frequently a trained radar observer can made this decision between rain types with no auxiliary information.

A result of this work, not anticipated, is that the drop size spectra can be represented by a log-normal distribution. This distribution contains three parameters rather than the two of prior distributions.

Recommendations for Future Study

Studies of these data are being continued in the following areas:

(a) The sample size necessary to adequately represent the parent drop size spectra

(b) The stratification of the remaining data by synoptic type

(c) Search for better criteria to perform the stratification

(d) Examine the relationships between the parameters of the log-normal fitting curve and rainfall rate.

With respect to (a), data were obtained in Illinois with two cameras located 37 meters apart and operating at 28 frames per minute. These data have been measured and the variances of the 1 m^3 samples are being calculated. The results should indicate the amount of reduction in size of the standard error of estimates which can be expected when volumes as large as a radar volume are considered.

With respect to (c), a number of criteria that might be considered are;

a) The amount of vertical wind shear

b) The level of the cloud base

c) Location of the point of interest with respect to storm center

d) Total depth of the cloud

e) The amount of moisture available to the storm

f) A combination of two or more criteria.

Plausible arguments can be given indicating that any of these might have an effect on the drop size spectra at the ground. In most cases, however, the necessary data to perform these stratifications are not available.

With respect to (d), the value of this study lies outside the radar application. This study may be important in the understanding of the precipitation process. Raindrop spectra may be an aid in evaluating cloud seeding experiments if sufficient knowledge of the natural spectra is available. The probable difference between the Alaska rains and the Marshall Island rains is that Alaskan hydrometeor growth is mostly as a snowflake while the Marshall Island growth is an all-liquid growth. Since silver iodide seeding is only effective in producing snowflakes, there is a chance that this would be reflected in the drop size spectra.

REFERENCES

1. Ryde, J. W., Echo Intensities and Attenuation Due To Clouds, Rain, Hall, Sand and Dust Storms, General Electric Co,, Rep. No. 7831, October 1941.

2. Bent, A. E., Radar Echoes from Atmospheric Phenomena, MIT Radiation Lab., Rep, No. 42-2, March 1943.

3. Marshall, J. S., R. C. Langille, and W, Palmer, "Measurement of Rainfall by Radar," J. of Meteor., 4:186-192, 1947.

4. Byers, H. R„, and collaborators, "The Use of Radar in Determining the Amount of Rain Palling Over a Small Area," Trans. A.G.U., 29:l87-196, 1948.

5. Atlas, D., Some Experimental Results of Quantitative Radar Analysis of Rain Storms, U.S.A.F., Air Material Command, May 194b.

6. Wexler, R., "Rain Intensities by Radar," J. of Meteor., 5:171-173, 1948.

7. Bemis, A. C, and collaborators, First Technical Report Under Signal Corps Project, Contract No. W-36-039 SC-32038, December 1946.

8. Lowe, E. J., "Raindrops," Quarterly J, Royal Meteor. Soc., 18:242-245, 1892.

9. Bentley, A., "Studies of Raindrops and Raindrop Phenomena," Monthly Weather Review, 32:450-456, October 1904.

10. Laws, J. 0., and D. A. Parsons, "The Relation of Raindrop Size to Intensity," Trans. A.G.U., 24:452-459, 1943.

11. Neuberger, H., "Notes on the Measurement of Raindrop Sizes," Bul. of A.M.S., 23:274-276, 1942.

12. Bowen, E. G., and K. A. Davidson, "A Raindrop Spectograph," Quarterly J. Royal Meteor. Soc., 7:445-449, 1951.

13. Cooper, B. F., "A Balloon-Borne Instrument for Telemetering Raindrop Size Distribution and Rainwater Content of Cloud," Australian J. of App. Science, 2:43-55, 1951.

14. Gucker, P. T., Jr., Determination of Concentration and Size of Particulate Matter by Light Scattering and Sonic Techniques, First National Air Pollution Symposium, Stanford Research Institute, Los Angeles, pp. 14-25, 1949.

15. Mason, B. J., and R. Ramanadham, "A Photoelectric Raindrop Spectrometer," Quarterly J. of Royal Meteor. Soc., 79:490-495, 1953.

16. Dingle, A. N., and J. P. Schulte, "A Research Instrument for the Study of Raindrop-Size Spectra," J. App. Meteor., 1:48-59, 1962.

17. Worthington, A. M., A Study of Splashes, Longmans, Green, 1908.

18. Edgerton, H. E., and J. R. Killian, Jr., Flash. Seeing the Unseen by Ultra High-Speed Photography, Hale, Cushman, and Flint, Boston, October 1939.

19. Best, A. C., The Shape of Raindrops and Mode of Disintegration of Large Drops, Meteorological Research Committee of Great Britain, MRP 330, 1947.

20. Elliot, H. W., Cloud Droplet Camera, National Res. Council of Canada, Rep. No. MI-701, December 1947.

21. Keily, D. P., Measurement of Drop Size Distribution and Liquid Water Content of Natural Clouds, MIT Quart. Prog. Rep. No. 5, Cont. No. AF 12(122)-245, 1951.

22. McCullough, S., and P. J. Perkins, Flight Camera for Photographing Cloud Droplets in Natural Suspension in the Atmosphere, National Advisory Committee of Aeronautics, Res. Mem. E50K0la, 1951.

23. Jones, D. M. A., and L. A. Dean, A Raindrop Camera, Ill. State Water Survey, Res. Rep, No. 3, Contract No. DA 36-039 SC-64723, 1953.

24. Pearson, J. E., and G. E. Martin, An Evaluation of Raindrop Sizing and Counting Techniques, Ill. State Water Survey, Scientific Rep. No. 1, Contract No. AF. 19(604)-1900, 1957.

25. Logan, N. A., "Survey of Some Early Studies of the Scattering of Plane Waves by a Sphere," Proc. of the I.E.E.E., 53-8:773-785, 1965.

26. Clebsch, A., "Ueber die Reflexion an einer Kugelfluche," J. fur Math., 61:195-262, 1863.

27. Lord Rayleigh, "On Scattering of Light by Small Particles," Phil. Ma,1., 41:447-454, 1871.

28. Lord Rayleigh, "Investigation of the Disturbance Produced by a Spherical Obstacle on the Waves of Sound," Proc. Math. Soc., 4:253-283, 1872.

29. Mie, G., "Beitrage zur Optik truber Medien, speziell kolloidaler Metallosungen," Ann. d. Physik, 25:377-442, 1908.

30. Stratton, J. A., Electromagnetic Theory, McGraw-Hill, N. Y., 1941.

31. Kerr, D. E., Editor, Propagation of Short Waves, MIT Rad. Lab., Vol. 13, McGraw-Hill, 1951.

32. Lowan, A., Editor, Tables of Scattering Functions for Spherical Particles, National Bureau of Standards, Washington, D. C, 1949.

33. Marshall, J. S., T. W. R. East, and K. L, S. Gunn, The Microwave Properties of Precipitation Particles, McGill Univ. Sci. Rep. MW-7 on Contract No. AF19(122)-217, 1952.

34. Kleinman, R. E.,"The Rayleigh Region," Proc. of I.E.E.E., 53:848-855, 1965.

35. Lawson, J. L., and G. E. Uhlenbeck, Threshold Signals, McGraw-Hill, N. Y., 1950.

36. Battan, L. J., Radar Meteorology, Univ. of Chi, Press, Chicago, Ill., 1959c

37. Hardy, A. C, and F. H. Perrin, The Principals of Optics, McGraw-Hill, N. Y., 1932.

38. Jones, D. M. A., "The Shape of Raindrops,'! J. of Meteor., 16:504-510, 1959.

39. Gunn, R., and G. D. Kinzer, "The Terminal Velocity of Fall for Water Droplets in Stagnant Air," J. of Meteor., 6:243-248, 1949.

40. Marshall, J. S„, and W. McK. Palmer, "The Distribution of Raindrops with Size," J. of Meteor., 4:186-192, 1947.

41. Fujiwara, M., Raindrop Size Distributions with Rainfall Types and Weather Conditions, Ill. State Water Survey, Res. Rep. No. 8, Contract No. DA-36-039 SC-87280, 1961.

42. Levine, L. M., "The Distribution Function of Cloud and Rain Drops by Sizes," Doklady Akad. Nauk., SSSR 94, No. 6, 1045-1048, 1954. (Translated by Assoc. Tech. Services Inc., East Orange, N. J.)

43. Matvejev, L. T., "On the Formation and Development of Layer Clouds," Tellus, 16:139-149, 1964.

44. Irani, R. R., and C. P. Callis, Particle Size: Measurement, Interpretation, and Application, John Wiley & Sons, N. Y., 1963.

45. Hitschfeld, W., and J. Bordan, Errors Inherent in the Radar Measurement of Rainfall at Attenuating Wavelengths, McGill Univ., Sci. Rep. No. MW-12, Contract AF 19(122)-217, 1953.

46. Robertson, S. D., and A. P. King, "The Effects of Rain Upon the Propagation of Waves in the 1- and 3-Centimeter Regions," Proc. I.R.E., 34:178-180, 1946.

DISTRIBUTION LIST

ADDRESSEE	NO. OF COPIES
Defense Documentation Center, ATTN: TISIA., Cameron Station (Bldg. 5), Alexandria, Virginia 22314	20
Commanding General, U. S. Army Materiel Command, ATTN: R&D Directorate, Washington, D. C. 20315	2
Office of Assistant Secretary of Defense, ATTN: Technical Library, Rm 3El065, Washington, D. C. 20301	2
Commanding Officer and Director, U. S. Navy Electronics Laboratory, ATTN: Library, San Diego, California 92101	1
Commander, Air Force Cambridge Research Laboratories, ATTN: CRXL-R L. G. Hanscom Field, Bedford, Massachusetts 01731	1
Air Weather Service (MAC) U. S. Air Force, ATTN: AWSSS/TIPD Scott Air Force Base, Illinois 62226	1
NASA Resresentative, Scientific and Technical Information Facility, P.O. Box 5700, Bethesda, Maryland 20014	1
Commanding General, U. S. Army Electronics Proving Ground ATTN: Technical Library, Fort Huachuca, Arizona 85613	1
Commanding General, U. S. Army Electronics Command, ATTN: AMSEL-BL-MA, Fort Monmouth, New Jersey 07703	5
Chief of Research and Development, Department of the Army ATTN: CRD/M, Washington, D. C. 20310	2
Commanding General, U. S. Army Electronics Command, ATTN: AMSEL-EW, Fort Monmouth, New Jersey 07703	1
Commanding General, U. S. Army Electronics Command, ATTN: AMSEL-IO-T, Fort Monmouth,New Jersey 07703	1
Commanding General, U. S. Army Electronics Command, ATTN: AMSEL-BL-D, Fort Monmouth, New Jersey 07703	1
Commanding General, U. S. Army Electronics Command, ATTN: AMSEL-RD-LNR, Fort MOnmouth, New Jersey 07703	1
Commanding General, U. S. Army Test and Evaluation Command, ATTN: AMSTE-EL, Aberdeen Proving Ground, Maryland 21005	1

ADDRESSEE	NO. OF COPIES
Commanding Officer, U. S. Array Research Support Group ATTN: CECMR-E, Fort Belvoir, Virginia 22060	1
Chief, Meteorology Division T&E Command, Dugway Proving Ground, Dugway, Utah	2
The American Meteorological Society, Abstracts & Bibliography P. 0. 1736, ATTN: Mr. M. Rigby, Washington, D. C.	1
Director, National Weather Records Center, Arcade Building ATTN: Mr. Haggard, Asheville, North Carolina	1
Brookhaven National Laboratories, Meteorological Department Camp Upton, New York	1
Climatic Center, U. S. Air Force, Annex 2, 225 D Street, S. E. Washington, D. C.	1
Commander, U. S. Army Artillery Combat Development Agency, Fort Sill, Oklahoma 73504	1
Commandant, U. S. Army Artillery & Missile School, ATTN: Target Acquisition Department, Fort Sill, Oklahoma 73504	1
President, U. S. Army Artillery Board, Fort Sill, Oklahoma 73504	1
Library, U. S. Weather Bureau, Washington, D. C.	1
Office of Technical Services, Department of Commerce, Washington, D. C.	1
Director, Atmospheric Sciences Programs, National Science Foundation, Washington, D. C.	1
Commanding Officer, U. S. Army Research & Development Group (Europe), ATTN: CRD-AF, APO New York 09757	1
Commander, U. S. Army Research Office (Durham) Box CM-Duke Station, Durham, North Carolina 27706	1
Director, Atmospheric Science & Chemistry Laboratory, ESSA, U. S. Weather Bureau, 24th & M Streets, N. W. Washington, D. C. 20235	1
Director, National Center for Atmospheric Research, Boulder, Colorado	1

ADDRESSEE	NO. OF COPIES
Officer-in-Charge, Meteorological Curriculum, U. S. Naval Research Facility, U. S. Naval Air Station, Bldg. B48, Norfolk, Virginia	1
Commanding General, U. S. Army Ordnance Missile Command, ATTN: ORDXM/RRA Dr. G. M. Essenwanger, Redstone Arsenal, Alabama	1
Director of Meteorology Research, ESSA, U. S. Weather Bureau, Washington, D. C.	1
Bureau of Ships Technical Library, ATTN: Code 312, Main Navy Building, Room 1528, Washington, D. C. 20325	1
Commanding Officer and Director, U. S. Navy Electronics Laboratory, ATTN: Library, San Diego, California 92152	1
Electronic Systems Division (AFSC), Scientific and Technical Info Div (ESTI), L. G. Hanscom Field, Bedford, Mass. 01731	1
Commanding General, U. S. Army Natick Laboratories, ATTN: Earth Sciences Division, Natick, Massachusetts	1
Chief, Bureau of Naval Weapons, Code FASS' Department of the Navy, Washington, D. C. 20316	1
Oregon State University, ATTN: Meteorological Department, Dr. Decker, Corvallis, Oregon	1
Commanding Officer, U. S. Army Combat Development Command, CBR Agency, Fort McClellen, Alabama 36205	1
Chief, Fallout Studies Branch, Division of Biology and Medicine, Atomic Energy Commission, Washington, D. C. 20315	1
Commanding General, U. S. Army Electronics Command, ATTN: AMSEL-RD-DR, Fort Monmouth, N.J. 07703	1
Commanding Officer, U. S. Army Electronics R&D Activity, ATTN: Chief, Atmospheric Science Research Division, SELHU-MM, Ft. Huachuca, Arizona 85613	2
Chief, Atmospheric Science Office, Atmospheric Sciences Laboratoryq U. S. Army Electronics Command, White Sands Missile Range, New Mexico 88002	2
Commanding General, U. S. Army Electronics Command, ATTN: AMSEL-RD-LNA, Fort Monmouth, New Jersey 07703	1

ADDRESSEE	NO. OF COPIES
Commanding General, U. S. Army Electronics Command, ATTN: AMSEL-RD-LNF, Fort Monmouth, New Jersey 07703	1
Commanding General, U. S. Army Electronics Command, ATTN: AMSEL-RD-MAF, Fort Monmouth, New Jersey 07703	1
U. S. National Bureau of Standards, ATTN: Technical Reports Laboratory, Washington, D. C. 20403	1
Department of Meteorology and Oceanography, New York University, College of Engineering, University Heights, New York 53, N. Y.	1
Department of Meteorology, Perm State Uriversity, 322 Mineral Industries Building, University Park, Penn. l6802	1
Dr. Edwin Kessler, Director, National Severe Storms Laboratory U. S. Weather Bureau, 1616 Holley Avenue, Norman, Oklahoma	1
Meteorology Department, Florida State University, ATTN: Dr. LaSeur, Tallahassee, Florida	1
Illinois State Water Survey, ATTN: Mr. Glenn Stout, Urbana, Illinois	1
Meteorology Department, University of Chicago, ATTN: Dr. Fugita, Chicago, Illinois	1
Dr. R. Cecil Gentry, Director, National Hurricane Research Laboratory, P. 0. Box 8265, Coral Gables, Florida 33124	1
Department of Meteorology, University of Miami, ATTN: Mr. Homer Hiser, Coral Gables, Florida	1

Security Classification

DOCUMENT CONTROL DATA - R&D

(Security classification of title body of abstract and indexing annotation must be entered when the overall report is classified)

1 ORIGINATING ACTIVITY (Corporate author)	2a REPORT SECURITY CLASSIFICATION
Illinois State Water Survey University of Illinois Urbana, Illinois	UNCLASSIFIED
	2b GROUP n/a

3 REPORT TITLE

Investigation of the Quantitative Determination of Point and Areal Precipitation by Radar Echo Measurements.

4 DESCRIPTIVE NOTES *(Type of report and inclusive dates)*

Final Report, 1 October 1964 to 30 September 1966

5 AUTHOR(S) *(Last name first name, initial)*

Mueller, E. A., and Sims, A. L.

6 REPORT DATE	7a TOTAL NO OF PAGES	7b NO OF REFS
December 1966	110	47

8a CONTRACT OR GRANT NO	9a ORIGINATOR'S REPORT NUMBER(S)
DA28-043 AMC-00032(E) b PROJECT NO 1VO-14501-B-53A-07 c d	9b OTHER REPORT NO(S) *(Any other numbers that may be assigned this report)* ECOM-00032-F

10 AVAILABILITY/LIMITATION NOTICES

Distribution of this document is unlimited

11 SUPPLEMENTARY NOTES	12 SPONSORING MILITARY ACTIVITY
None	U, S. Army Electronics Command Fort Monmouth New Jersey 07703 AMSEL-PL-AP

13 ABSTRACT

A review of work accomplished on this contract is presented including references to the appropriate interim reports for details. The limiting accuracy for radar estimation of rainfall rate is determined to be ±40 percent.

The location of the medium range raingage network is shown along with the amount of data collected thus far. No results from this network are available at present.

A Doctoral thesis entitled, "Radar Cross Sections from Drop Size Spectra," is included as an Appendix.

DD FORM 1 JAN 64 1473

Security Classification

14 KEY WORDS	LINK A		LINK B		LINK C	
	ROLE	WT	ROLE	WT	ROLE	WT
precipitation radar measurements raindrop size distribution rainfall rate weather radar						

INSTRUCTIONS

1 ORIGINATING ACTIVITY Enter the name and address of the contractor, subcontractor, grantee, Department of Defense activity or other organization *(corporate author)* issuing the report

2a REPORT SECURITY CLASSIFICATION Enter the overall security classification of the report Indicate whether "Restricted Data" is included. Marking 16 to be ln-accordance with appropriate security regulations

26 GROUP Automatic downgrading is specified in DoD Directive 5200 10 and Armed Forces Industrial Manual Enter the group number Also, when applicable, show that optional markings have been used for Group 3 and Group 4 as authorized

3 REPORT TITLE Enter the complete report title in all capital letters Titles in all cases should be unclassified If a meaningful title cannot be selected without classification, show title classification in all capitals in parenthesis immediately following the title.

4 DESCRIPTIVE NOTES ff appropriate, enter the typeof report, e g , interim, progress, summary, annual, or final Give the inclusive dates when a specific reporting period is covered

5 AUTHOR(S) Enter the name(s) of author(s) as shown on or in the report Enter last name, first name, middle initial If military, show rank and branch of service The name of the principal author is an absolute minimum requirement

6 REPORT DATE. Enter the date of the report as day, month, year, or month, year. If more than one date appears on the report, use date of publication.

la TOTAL NUMBER OF PAGES The total page count should follow normal pagination procedures, i e., enter the number of pages containing information.

76 NUMBER OF REFERENCES. Enter the total number of references cited in the report

8a CONTRACT OR GRANT NUMBER If appropriate, enter the applicable number of the contract or grant under which the report was written.

86, 8c, & 8d PROJECT NUMBER Enter the appropriate military department identification, such as project number, subproject number, system numbers, task number, etc.

9a ORIGINATOR'S REPORT NUMBER(S) Enter the official eport number by which the document will be identified and controlled by the originating activity This number must be unique to this report

96 OTHER REPORT NUMBER(S) If the report has been assigned any other report numbers *(either by the originator or by the sponsor),* also enter this number(s)

10 AVAILABILITY/LIMITATION NOTICES Enter any limitations on further dissemination of the report, other than those imposed by security classification, using standard statements such as

(1) "Qualified requesters may obtain copies of this report from DDC"

(2) "Foreign announcement and dissemination of this report by DDC is not authorized "

(3) "U S Government agencies may obtain copies of this report directly from DDC. Other qualified DDC users shall request through _____ "

(4) "U S military agencies may obtain copies of this report directly from DDC Other qualified users , shall request through _____ "

(5) "All distribution of this report is controlled. Qualified DDC users shall request through _____ "

If the report has been furnished to the Office of Technical Services, Department of Commerce, fer sale to the public, indicate this fact and enter the price, if known.

11 SUPPLEMENTARY NOTES Use for additional explanatory notes.

12 SPONSORING MILITARY ACTIVITY Enter the name of the departmental project office or laboratory sponsoring *(paying* for) the research and development. Include address

13 ABSTRACT Enter an absracr giving a brief and factual summary of the document indicative of the report, even though it may also appear elsewhere in the body of the technical report If additional space is required, a continuation sheet shall be attached

It is highly desirable that the abstract of classified reports be unclassified Each paragraph of the abstract shall end with an indication of the military security classification of the information in the paragraph, represented as *(TS), (S), (C), or (U)*

There is no limitation on the length of the abstract However, the suggested length is from 150 to 225 words

14 KEY WORDS Key words are technically meaningful terms or short phrases that characterize a report and may be used as index entries for cataloging the report Key words must be selected so that no security classification is required Idenfiers, such as equipment model designation, trade name, military project code name, geographic location, may be used as key words but will be followed by an indication of technical context The assignment of links, rules, and weights is optional